CONVERGENCE ANALYSIS OF FULLY DISCRETE FINITE VOLUME METHODS FOR MAXWELL'S EQUATIONS IN NON-HOMOGENEOUS MEDIA

ERIC T. CHUNG * AND BJORN ENGQUIST †

Abstract. We will consider both explicit and implicit fully discrete finite volume schemes for solving the three dimensional Maxwell's equations with discontinuous physical coefficients on general polyhedral domains. Stability and convergence for both schemes are analysed. We prove that the schemes are second order accurate in time. Both schemes are proved to be first order accurate in space for general unstructured grids and second order accurate for non-uniform rectangular grids. We also derive explicit expressions for the dependence on the physical parameters in all estimates and discuss the relation between finite volume and finite element methods.

1. Introduction. The finite volume method (FVM) has been developed as a practical compromize between the finite difference method (FDM) and the finite element method (FEM) in the numerical solutions of electromagnetic problems, [1, 2, 9, 10, 12, 20, 22, 23]. It allows for unstructured grids, as the FEM does, but it is typically explicit and as computationally efficient as the FDM.

Even though finite element methods provide excellent tools for solving electromagnetic problems on geometrically complex domains, marching technques applied to finite element methods produce implicit schemes. At every time step, the mass matrix has to be inverted. For certain quadrature rules the mass matrix will be diagonal. We will discuss the relation between such methods and finite volume methods in section 6. In order to obtain an explicit scheme to solve Maxwell's equations on domains which are geometrically complicated, finite volume methods are considered. There are many different finite volume methods for solving Maxwell's equations. We will give a brief overview of those which are popular in the computational electromagnetic community. But let us first introduce notations and formulate the differential equations to be approximated. Let Ω be a general polyhedral domain in $\mathbb{R}^3$, and occupied by a material with the electric permittivity ε and the magnetic permeability μ. The Maxwell's equations can be described as follows:

$$\varepsilon\frac{\partial \mathbf{E}}{\partial t} - \mathbf{curl}\ \mathbf{H} = \mathbf{J} \quad \text{in} \quad \Omega\times(0,T), \tag{1.1.1}$$

$$\mu\frac{\partial \mathbf{H}}{\partial t} + \mathbf{curl}\ \mathbf{E} = 0 \quad \text{in} \quad \Omega\times(0,T), \tag{1.1.2}$$

$$\operatorname{div}(\varepsilon\mathbf{E}) = \rho \quad \text{in} \quad \Omega\times(0,T), \tag{1.1.3}$$

$$\operatorname{div}(\mu\mathbf{H}) = 0 \quad \text{in} \quad \Omega\times(0,T), \tag{1.1.4}$$

where $\mathbf{E}=\mathbf{E}(\mathbf{x},t)$ and $\mathbf{H}=\mathbf{H}(\mathbf{x},t)$ denote the electric and magnetic fields, $\mathbf{J}=\mathbf{J}(\mathbf{x},t)$ the applied current density and $\rho=\rho(\mathbf{x},t)$ the charge density. The paper is concerned with the case where the domain Ω is composed of two distinct dielectric materials. Let Ω_1 be a polyhedral subdomain strictly lying inside Ω and occupied by a material with the electric permittivity ε_1 and the magnetic permeability μ_1, and let $\Omega_2=\Omega\backslash\bar{\Omega}_1$ be occupied by another material with the electric permittivity ε_2 and the magnetic permeability μ_2. For ease of exposition, we shall consider only the case that the

*Department of Mathematics, University of California, Los Angeles, CA 90095, USA. (tschung@math.ucla.edu).

†PACM, Department of Mathematics, Princeton University, Princeton, NJ 08544, USA. (engquist@math.princeton.edu).

parameters ε_i and μ_i are constant functions in Ω_i, $i = 1, 2$, but with possibly great differences in their values. We remark that our subsequent analysis can be naturally extended to the case with piecewise smooth coefficients as well as multiple subdomains for which our methods have broad applications [1, 10].

Let $\Gamma = \partial\Omega_1$ be the boundary of Ω_1 with a unit outward normal vector $\mathbf{m}$, and $\partial\Omega$ be the boundary of Ω with a unit outward normal vector $\mathbf{n}$, see Figure 1. We supplement the system (1.1.1)-(1.1.4) with the perfect conductor boundary condition and the initial condition given by

$$\mathbf{E} \times \mathbf{n} = 0 \quad \text{on} \quad \partial\Omega \times (0, T) \tag{1.1.5}$$

$$\mathbf{E}(\mathbf{x}, 0) = \mathbf{E}_0(\mathbf{x}) \quad \text{and} \quad \mathbf{H}(\mathbf{x}, 0) = \mathbf{H}_0(\mathbf{x}) \;, \quad \forall x \in \Omega. \tag{1.1.6}$$

It is well-known [1] [21] that the electric and magnetic fields $\mathbf{E}$ and $\mathbf{H}$ satisfy the following physical jump conditions across the interface Γ:

$$[\mathbf{E} \times \mathbf{m}] = 0 \quad , \quad [\varepsilon \mathbf{E} \cdot \mathbf{m}] = \rho_\Gamma, \tag{1.1.7}$$

$$[\mathbf{H} \times \mathbf{m}] = 0 \quad , \quad [\mu \mathbf{H} \cdot \mathbf{m}] = 0, \tag{1.1.8}$$

where $\rho_\Gamma(\mathbf{x})$ is the surface charge density and, throughout the paper, the jump of any function f across the interface Γ is defined by

$$[f] := f_2|_\Gamma - f_1|_\Gamma$$

where $f_i = f|_{\Omega_i}$ for $i = 1, 2$.

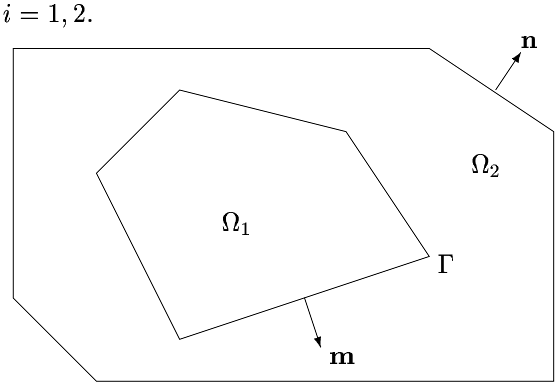

Figure 1: 2D cross-section of dielectric materials Ω_1, Ω_2 and their interface Γ

In addition, we have the following constitutive relations

$$\mathbf{D} = \varepsilon \mathbf{E} \quad , \quad \mathbf{B} = \mu \mathbf{H} \quad , \tag{1.1.9}$$

where $\mathbf{D}$ and $\mathbf{B}$ are the electric flux density and the magnetic flux density respectively.

First of all, we notice that (1.1.1)-(1.1.2) can be written as a system of first order hyperbolic equations in conservation form. One way to solve (1.1.1)-(1.1.2) is to apply numerical techniques for solving general hyperbolic systems. Stability of these schemes is often obtained by using dissipative time marching methods. For general overview of finite volume methods for hyperbolic systems, see Leveque [11]. For a comparative study of finite difference method and this kind of finite volume method, the reader is referred to Jensen and Rahmat-Samii [9].

A finite volume method based on hybrid grid is introduced by Riley and Turner [20]. Primal grid is a set of tetrahedra triangulating a given domain. Dual grid is formed by connecting barycenters of adjacent tetrahedra. Let V and V' be an element of primal grid and dual grid respectively. Then the finite volume method in Riley and Turner [20] is derived based on the following integral form of (1.1.1)-(1.1.2):

$$\mu \int_V \frac{\partial \mathbf{H}}{\partial t}\, dx + \int_{\partial V} \mathbf{E} \times \mathbf{n}\, d\sigma = 0,$$
$$\varepsilon \int_{V'} \frac{\partial \mathbf{E}}{\partial t}\, dx - \int_{\partial V'} \mathbf{H} \times \mathbf{n}\, d\sigma = \int_{V'} \mathbf{J}\, dx.$$

The unknown of $\mathbf{H}$ is defined at the barycenter of primal element while the unknown of $\mathbf{E}$ is defined at the barycenter of dual element. So, the volume integrals in the above two equations can be evaluated by using values at the barycenters. Notice that ∂V and $\partial V'$ are union of polygons. So, the surface integrals in the above two equations can be evaluated by using the values at the corners of each polygon. A FDTD correction term is added to ensure the numerical solution satisfies the two divergence constraints (1.1.3)-(1.1.4) in some discrete sense. This scheme exhibits late time instability. A dissipative version of leap-frog time discretization is applied to solve this problem. Due to the complexity of this scheme, the reader is referred to Riley and Turner [20] for details of this scheme. Stability and convergence analysis of this scheme are still open problems.

A different type of finite volume method, based on surface integrals rather than volume integrals as in Riley and Turner [20], is introduced by Madsen [12]. A set of polyhedra, called primal cells are used to triangulate a given domain. Dual cells are formed by connecting barycenters of adjacent primal cells. The scheme is to find the electric field component projected to each dual edge while the magnetic field component projected to each primal edge. This scheme is second order accurate both in space and time. Moreover, divergence is preserved both locally and globally. As compared to the above two types of finite volume method, this method provides a non-dissipative scheme. However, convergence and stability analysis of this scheme are still open problems. One variant of this type of finite volume method, with the use of circumcenter instead of barycenter as in Madsen [12], was suggested in Chen and Yee [2]. Convergence analyses for both semi-discrete and fully-discrete schemes were given by Nicolaides and Wang [18].

There has been serious stability problems with some FVM approximations of the Maxwell's equations. In this paper we will present a class of FVMs for which we prove stability and convergence. We will in particular consider inhomogeneous media with discontinuous coefficients. The methods presented here are based on the semi-discrete techniques introduced by Chung and Zou [4] and Chung, Du and Zou [5].

The rest of the paper is organized as follows. In section 2, we will introduce notations for function spaces that are used throughout the paper. We will also define discrete vector spaces that are used to define the finite volume approximations. Some mesh and parameter dependent inner products and norms are also defined in this section. In section 3, we will briefly derive the finite volume spatial discretization of Maxwell's equations. In section 4, we will derive both explicit and implicit fully discrete finite volume schemes. They are based on leap-frog and Crank-Nicolson time discretization respectively. Convergence and stability will be analysed in case of general tetradedral grids. In section 5, we extend the schemes to non-uniform rectangular grids. It can be shown that the spatial convergence is one order higher. We will also provide an example in one space dimension to show the optimality of our estimates from section 5. We will discuss a relationship between finite volume method and linear edge element method for Maxwell's equations in section 6.

2. Functions and discrete vector spaces. We start this section with some notations to be used in the subsequent analysis. For a nonnegative integer m and $1 \leq p < \infty$, we use $W^{m,p}(\Omega)$ to denote the standard Sobolev space equipped with the norm $\|u\|_{W^{m,p}(\Omega)} = (\sum_{0\leq|\alpha|\leq m} \|D^\alpha u\|^p_{L^p(\Omega)})^{1/p}$ and the semi-norm $|u|_{W^{m,p}(\Omega)} = (\sum_{|\alpha|=m} \|D^\alpha u\|^p_{L^p(\Omega)})^{1/p}$. Here $D^\alpha u$ denotes the α-th order weak derivative of u. Furthermore, for some $0 < \lambda < 1$, $u \in C^{m,\lambda}(\Omega)$ denotes the standard Holder spaces of functions whose m-th order derivatives are Holder continuous with exponent λ. Note that same definitions are adopted for Ω_1 and Ω_2.

We use $L^p(0,T;\mathbf{X})$ to denote the space of all L^p integrable functions $\mathbf{u}(t,\cdot)$ from $[0,T]$ into the Banach space $\mathbf{X}$, and we also define

$$W^{m,p}(0,T;\mathbf{X}) = \Big\{\mathbf{u} \in L^p(0,T;\mathbf{X}) \quad ; \quad \frac{\partial^\alpha \mathbf{u}}{\partial t^\alpha} \in L^p(0,T;\mathbf{X}) \quad \forall|\alpha| \leq m\Big\},$$

with norm

$$\|\mathbf{u}\|_{W^{m,p}(0,T;\mathbf{X})} = \Big\{\sum_{0\leq|\alpha|\leq m} \|\frac{\partial^\alpha \mathbf{u}}{\partial t^\alpha}\|^p_{\mathbf{X}}\Big\}^{1/p}.$$

When $p = 2$, we set $H^m(\Omega) = W^{m,2}(\Omega)$ and $H^m(0,T;\mathbf{X}) = W^{m,2}(0,T;\mathbf{X})$.

We now discuss the triangulation of the domain Ω. We use the Voronoi-Delaunay triangulation (cf. [7]), which enjoys many elegant geometric properties that allow us to derive the numerical schemes in the subsequent sections. We first triangulate Ω using the standard tetrahedral cells, which are called the *primal elements*. The triangulation is chosen so that the faces of the primal elements align with the interface Γ. A primal element with at least one face lying on Γ is called an *interface primal element*, and a primal face (edge) lying on Γ is called an interface primal face (edge).

The *dual elements* are the Voronoi polyhedras formed by connecting the circumcenters of adjacent primal elements. Those dual elements (faces and edges) separated by the interface Γ into two parts lying respectively in Ω_1 and Ω_2 are called the interface dual elements (faces and edges). The definitions and convergence analysis related to dual elements are much more complicated than those related to primal elements due to the interface. From geometry, it is known that each primal edge is perpendicular to and in one-to-one correspondence with a dual face, and each dual edge is perpendicular to and in one-to-one correspondence with a primal face.

For the subsequent convergence analysis, we assume that all dihedral angles of each tetrahedron are uniformly acute and the triangulation restricted in each subdomain satisfies

$$K_r \leq \frac{h^r_{\max}}{h^r_{\min}} \leq \tilde{K}_r, \quad r = 1, 2 \tag{2.2.1}$$

where $h^r_{\max}$ and $h^r_{\min}$ are, respectively, the local maximum and minimum side lengths of adjacent primal and dual elements in Ω_r, K_r and $\tilde{K}_r$ are two positive constants. Throughout this paper, K represents a generic constant which is independent of the mesh size and the physical coefficients ε and μ, but with the possibility that it may depends on K_r or $\tilde{K}_r$.

Let N and L be the numbers of primal and dual elements respectively, and F be the number of primal faces (dual edges) and M the number of primal edges (dual faces). Assume that these quantities are numbered sequentially in some order. The individual elements, faces, edges and nodes of the primal mesh are denoted by τ_i, κ_j, σ_k and ν_l respectively. Those quantities related to the dual mesh are denoted by the primed forms such as τ_i', κ_j', σ_k' and ν_l'. A direction is assigned to each primal and dual edge by the rule that positive direction is from low to high node number. Direction is also assigned to each primal (dual) face such that it is the same as the corresponding dual (primal) edge. We denote by F_1 the number of interior primal faces (dual edges) and M_1 the number of interior primal edges (dual faces). For each dual edge σ_j' of length h_j', we define a scaled length:

$$\bar{h}_j' = \begin{cases} \frac{1}{\mu_1} h_j' & \text{if} \quad \sigma_j' \in \Omega_1 \\ \frac{1}{\mu_2} h_j' & \text{if} \quad \sigma_j' \in \Omega_2 \\ (\frac{1}{\mu_1} a_j + \frac{1}{\mu_2}(1-a_j))h_j' & \text{otherwise,} \end{cases}$$

where $0 < a_j < 1$ is the ratio of the length of the portion of σ_j' that belongs to Ω_1 over the length of σ_j'. For any u and v in $\mathbb{R}^{F_1}$, we introduce a mesh and parameter depending inner product defined by

$$(u,v)_W := \sum_{\kappa_j \subset \Omega} u_j v_j s_j \bar{h}_j' = (Su, D'v) = (D'u, Sv), \tag{2.2.2}$$

where $S := \text{diag}(s_j)$ and $D' := \text{diag}(\bar{h}_j')$ are $F_1 \times F_1$ diagonal matrices, $(\cdot,\cdot)$ denotes the standard Euclidean inner product. Similarly, for each dual face κ_j' with area s_j', we define a scaled area:

$$\bar{s}_j' = \begin{cases} \varepsilon_1 s_j' & \text{if} \quad \kappa_j' \in \Omega_1 \\ \varepsilon_2 s_j' & \text{if} \quad \kappa_j' \in \Omega_2 \\ (\varepsilon_1 b_j + \varepsilon_2(1-b_j))s_j' & \text{otherwise,} \end{cases}$$

where $0 < b_j < 1$ is the ratio of the area of the portion of κ_j' that belongs to Ω_1 over the area of κ_j'. Also, we define a mesh and parameter depending inner product in $\mathbb{R}^{M_1}$ by

$$(u,v)_{W'} := \sum_{\kappa_j' \subset \Omega} u_j v_j \bar{s}_j' h_j = (S'u, Dv) = (Du, S'v), \tag{2.2.3}$$

where $S' := \text{diag}(\bar{s}_j')$ and $D := \text{diag}(h_j)$ are $M_1 \times M_1$ diagonal matrices.

For any $\sigma_j \in \partial\kappa_i$, we say σ_j is oriented positively along $\partial\kappa_i$ if the direction of σ_j agrees with the one of $\partial\kappa_i$ formed by the right hand rule with the thumb pointing to the direction of σ_i'. Otherwise, we say σ_j is oriented negatively along $\partial\kappa_i$. For each interior primal face κ_i, we define its discrete circulation by

$$(Cu)_{\kappa_i} := \sum_{\sigma_j \subset \partial\kappa_i} u_j \tilde{h}_j, \tag{2.2.4}$$

where

$$\tilde{h}_j = \begin{cases} h_j & \text{if } \sigma_j \text{ is oriented positively along } \partial\kappa_i \\ -h_j & \text{if } \sigma_j \text{ is oriented negatively along } \partial\kappa_i. \end{cases}$$

Similarly, for each interior dual face κ'_i we define its discrete circulation by

$$(C'u)_{\kappa'_i} := \sum_{\sigma'_j \subset \partial\kappa'_i} u_j \tilde{h}'_j, \tag{2.2.5}$$

where

$$\tilde{h}'_j = \begin{cases} \bar{h}'_j & \text{if } \sigma'_j \text{ is oriented postively along } \partial\kappa'_i \\ -\bar{h}'_j & \text{if } \sigma'_j \text{ is oriented negatively along } \partial\kappa'_i. \end{cases}$$

Clearly, C and C' are two linear mappings from $\mathbb{R}^M$ to $\mathbb{R}^{F_1}$ and $\mathbb{R}^{F_1}$ to $\mathbb{R}^{M_1}$ respectively. We remark that (2.2.4) and (2.2.5) are the discrete analogs of the integrals

$$\int_{\kappa_i} (\mathbf{curl\,E}) \cdot \mathbf{n}\, d\sigma \quad \text{and} \quad \int_{\kappa'_i} (\mathbf{curl\,H}) \cdot \mathbf{n}\, d\sigma$$

by the Stokes' theorem, where and in what follows $\mathbf{n}$ represents the unit normal vector to both primal and dual faces.

For each strictly interior dual edge σ'_j with both end points of σ'_j lying in Ω and the ith strictly interior dual face κ'_i, we define the entries of a $F_1 \times M_1$ matrix G as:

$$(G)_{ji} := \begin{cases} 1 & \text{if } \sigma'_j \text{ is oriented positively along } \partial\kappa'_i \\ -1 & \text{if } \sigma'_j \text{ is oriented negatively along } \partial\kappa'_i \\ 0 & \text{if } \sigma'_j \text{ does not meet } \partial\kappa'_i. \end{cases}$$

Let $w \in \mathbb{R}^M$ be a vector whose kth component is the value assigned on the kth primal edge. Let $w_1 \in \mathbb{R}^{M_1}$ be the restriction of w to the interior primal edges. Denote by $w|_{\partial\Omega}$ the components of w that are related to the boundary. Likewise, denote by $v \in \mathbb{R}^{F_1}$ the vector whose jth component represents a value on the jth interior dual edge. Proved in [5], we have:

LEMMA 2.1. *Let w, w_1 and v be defined as above, and $w|_{\partial\Omega} = 0$, then we have*

$$Cw = GDw_1 \quad \text{and} \quad C'v = G^T D'v. \tag{2.2.6}$$

Using lemma 2.1, we can show a discrete analog of the following Green's formula

$$\int_\Omega \mathbf{curl\,E} \cdot \mathbf{B}\, dx = \int_\Omega \mathbf{curl\,B} \cdot \mathbf{E}\, dx$$

which holds when $\mathbf{E} \times \mathbf{n} = 0$ on $\partial\Omega$: (cf. [5])

LEMMA 2.2. *Under the same definitions as in lemma 2.1, we have*

$$(Cw, D'v) = (C'v, Dw_1) \tag{2.2.7}$$

3. The finite volume method. The finite volume method proposed in Chung and Zou [4] for solving the interface Maxwell's equations (1.1.1)-(1.1.8) approximates the edge average of $\mathbf{E}$ on each primal edge and the face average of $\mathbf{B}$ on each primal face. The use of the magnetic flux density $\mathbf{B}$ in the approximation, instead of the magnetic field $\mathbf{H}$ as used in most existing numerical methods, is crucial for maintaining a good order accuracy in the interface problems.

We now introduce some average quantities. For the magnetic flux density $\mathbf{B}$, we define its primal face average $B_f \in \mathbb{R}^{F_1}$ by

$$(B_f)_i := \frac{1}{s_i} \int_{\kappa_i} \mathbf{B} \cdot \mathbf{n}_i \, d\sigma$$

for each primal face κ_i, and its dual edge average $B'_e \in \mathbb{R}^{F_1}$ by

$$(B'_e)_i := \frac{1}{h'_i} \int_{\sigma'_i} \mathbf{B} \cdot \mathbf{t}_i \, dl$$

for each non-interface dual edge σ'_i and

$$\begin{aligned} (B'_e)_i &:= \alpha_i (B'_{e_1}) i + (1-\alpha_i)(B'_{e_2})_i \\ &:= \alpha_i \frac{1}{h^1_i} \int_{\sigma^1_i} \mathbf{B} \cdot \mathbf{t}_i \, dl + (1-\alpha_i) \frac{1}{h^2_i} \int_{\sigma^2_i} \mathbf{B} \cdot \mathbf{t}_i \, dl \end{aligned} \tag{3.3.1}$$

for each interface dual edge σ'_i. Here $\sigma^1_i = \sigma'_i \cap \Omega_1$ and $\sigma^2_i = \sigma'_i \cap \Omega_2$ are the portions of σ'_i in Ω_1 and Ω_2 respectively, and $\alpha_i := \mu_1^{-1} h^1_i (\bar{h}'_i)^{-1}$ with h^r_i being the length of σ^r_i for $r = 1, 2$.

For the electric field $\mathbf{E}$, we define its primal edge average $E_e \in \mathbb{R}^{M_1}$ by

$$(E_e)_i := \frac{1}{h_i} \int_{\sigma_i} \mathbf{E} \cdot \mathbf{n}_i \, dl$$

for each primal edge σ_i, and its dual face average $E'_f \in \mathbb{R}^{M_1}$ by

$$(E'_f)_i := \frac{1}{s'_i} \int_{\kappa'_i} \mathbf{E} \cdot \mathbf{n}_i \, d\sigma$$

for each non-interface dual face κ'_i and

$$\begin{aligned} (E'_f)_i &:= \beta_i (E'_{f_1})_i + (1-\beta_i)(E'_{f_2})_i \\ &:= \beta_i \frac{1}{s^1_i} \int_{\kappa^1_i} \mathbf{E} \cdot \mathbf{n}_i \, d\sigma + (1-\beta_i) \frac{1}{s^2_i} \int_{\kappa^2_i} \mathbf{E} \cdot \mathbf{n}_i \, d\sigma \end{aligned} \tag{3.3.2}$$

for each interface dual face κ'_i. Here $\kappa^1_i = \kappa'_i \cap \Omega_1$ and $\kappa^2_i = \kappa'_i \cap \Omega_2$ are the portions of κ'_i in Ω_1 and Ω_2 with their areas being s^1_i and s^2_i respectively, and $\beta_i := \varepsilon_1 s^1_i (\bar{s}'_i)^{-1}$.

For each primal face κ_j and each dual face κ'_j, we have [4]:

$$s_j \frac{d}{dt}(B_f)_j + (CE_e)_{\kappa_j} = 0; \tag{3.3.3}$$

$$\bar{s}'_j \frac{d}{dt}(E'_f)_j - (C'B'_e)_{\kappa'_j} = \int_{\kappa'_j} \mathbf{J} \cdot \mathbf{n} \, d\sigma \, ; \tag{3.3.4}$$

Let $E \in \mathbb{R}^{M_1}$ and $B \in \mathbb{R}^{F_1}$ be the approximations of the primal edge and face averages of the true solution $\mathbf{E}$ and $\mathbf{B}$ to (1.1.1)-(1.1.4) respectively. Note that each dual face (edge) average and the corresponding primal edge (face) average are approximately the same for sufficiently small h. Due to continuity of the tangential component of $\mathbf{E}$ and the normal component of $\mathbf{B}$ across the interface Γ, we naturally come to the following approximations based on (3.3.3) and (3.3.4):

Find $E \in \mathbb{R}^{M_1}$ and $B \in \mathbb{R}^{F_1}$ such that

$$S' \frac{dE}{dt} - C'B = \tilde{J}, \tag{3.3.5}$$

$$S \frac{dB}{dt} + CE = 0 \tag{3.3.6}$$

where $\tilde{J} \in \mathbb{R}^{M_1}$ is defined by the right-hand side of (3.3.4). Convergence and stability analysis of the semi-discrete scheme (3.3.5)-(3.3.6) was given in Chung, Du and Zou [5]. In the following sections, we will consider time discretizations of the semi-discrete scheme (3.3.5)-(3.3.6).

4. Fully discrete schemes. In this section, we will give two different time discretizations for (3.3.5)-(3.3.6). First, we will consider an explicit scheme, which is a standard leapfrog scheme. With a stability condition, this scheme can be shown to be first order convergent in space and second order convergent in time. Secondly, we will consider an implicit scheme, which is a Crank-Nicolson time discretization of (3.3.5)-(3.3.6). It can be shown that this method is unconditionally stable with the same rate of convergence as the explicit counterpart.

Consider a uniform partition of $[0, T]$ with N_T subintervals. Let $\Delta t := T/N_T$. For $n = 0, 1, \cdots, N_T - 1$, we define $t_n := n\Delta t$ and $t_{n+\frac{1}{2}} := (n + \frac{1}{2})\Delta t$. For subsequent analysis, we define

$$c_m := (\min(\varepsilon_1, \varepsilon_2) \min(\mu_1, \mu_2))^{-\frac{1}{2}}.$$

We also denoted by M_2 the maximum of the ratios of maximum to minimum side lengths over adjacent tetrahedra and by M_3 the maximum number of sides over all dual faces. Furthermore, by $\min(h)$ we mean the minimum side length over all primal and dual edges.

4.1. Explicit scheme. We will apply a leapfrog scheme to (3.3.5)-(3.3.6). We approximate $\mathbf{E}(t)$ at t_n and $\mathbf{B}(t)$ at $t_{n+\frac{1}{2}}$ with approximations denoted by E^n and $B^{n+\frac{1}{2}}$ respectively. Given $(E^n, B^{n+\frac{1}{2}})$, the next approximation $(E^{n+1}, B^{n+\frac{3}{2}})$ will be obtained by solving

$$S'(E^{n+1} - E^n) - \Delta t C' B^{n+\frac{1}{2}} = \tilde{J}^{n+\frac{1}{2}}, \tag{4.4.1}$$

$$S(B^{n+\frac{3}{2}} - B^{n+\frac{1}{2}}) + \Delta t C E^{n+1} = 0, \tag{4.4.2}$$

where

$$\tilde{J}^{n+\frac{1}{2}} := \int_{n\Delta t}^{(n+1)\Delta t} \tilde{J}(s)\, ds.$$

Now, we have the following stability estimate.

THEOREM 4.1. *Under the stability condition*

$$\delta := \Delta t c_m \frac{M_2^{\frac{3}{2}} M_3^{\frac{1}{2}}}{\min(h)} < 1, \tag{4.4.3}$$

the fully discrete scheme (4.4.1)-(4.4.2) is stable. Moreover, the following stability estimate holds for $1 \le k \le N_T - 1$*:*

$$\|E^k\|_{W'}^2 + \|B^{k+\frac{1}{2}}\|_W^2 \le \frac{2(1+\delta)}{1-\delta}(\|E^0\|_{W'}^2 + \|B^{\frac{1}{2}}\|_W^2) + \frac{4T}{(1-\delta)^2}\int_0^T \|S^{'-1}\tilde{J}(t)\|_{W'}^2\, dt. \tag{4.4.4}$$

Proof. Multiplying (4.4.1) by $D(E^{n+1}+E^n)$ and (4.4.2) by $D'(B^{n+\frac{3}{2}}+B^{n+\frac{1}{2}})$ yields

$$(E^{n+1}-E^n, E^{n+1}+E^n)_{W'} - \Delta t(C'B^{n+\frac{1}{2}}, D(E^{n+1}+E^n)) = R^{n+\frac{1}{2}},$$
$$(B^{n+\frac{3}{2}}-B^{n+\frac{1}{2}}, B^{n+\frac{3}{2}}+B^{n+\frac{1}{2}})_W + \Delta t(CE^{n+1}, D'(B^{n+\frac{3}{2}}+B^{n+\frac{1}{2}})) = 0.$$

where $R^{n+\frac{1}{2}} := (\tilde{J}^{n+\frac{1}{2}}, D(E^{n+1}+E^n))$. Let k be an integer satisfying $1 \le k \le N_T - 1$. Adding all equations from $n=0$ to $n=k-1$ and using (2.2.7), we have

$$\begin{aligned}&\|E^k\|_{W'}^2 + \|B^{k+\frac{1}{2}}\|_W^2\\ &= \|E^0\|_{W'}^2 + \|B^{\frac{1}{2}}\|_W^2 + \Delta t(C'B^{\frac{1}{2}}, DE^0) - \Delta t(CE^k, D'B^{k+\frac{1}{2}}) + \sum_{n=0}^{k-1} R^{n+\frac{1}{2}}.\end{aligned} \tag{4.4.5}$$

Notice that

$$\Delta t(C'B^{\frac{1}{2}}, DE^0) \le \Delta t\|(DS^{'-1})^{\frac{1}{2}}C'(SD')^{-\frac{1}{2}}\|_2\|B^{\frac{1}{2}}\|_W\|E^0\|_{W'}.$$

By Gershgorin's theorem, the 2-norm of a matrix is bounded above by the maximum of row sums over each row of the matrix. So,

$$\|(DS^{'-1})^{\frac{1}{2}}C'(SD')^{-\frac{1}{2}}\|_2 \le c_m \max_{1\le j\le M_1}(\frac{\max_j(h)^{\frac{3}{2}}}{\min_j(h)^{\frac{5}{2}}})(2M_3^{\frac{1}{2}}),$$

where $\max_j(h)$ and $\min_j(h)$ are the local maximum and local minimum of side lengths around a dual face κ'_j respectively. So, we have

$$\Delta t(C'B^{\frac{1}{2}}, DE^0) \le \Delta t c_m \frac{M_2^{\frac{3}{2}}M_3^{\frac{1}{2}}}{\min(h)}(\|B^{\frac{1}{2}}\|_W^2 + \|E^0\|_{W'}^2).$$

Similiarly, we have

$$\Delta t(C'B^{k+\frac{1}{2}}, DE^k) \le \Delta t c_m \frac{M_2^{\frac{3}{2}}M_3^{\frac{1}{2}}}{\min(h)}(\|B^{k+\frac{1}{2}}\|_W^2 + \|E^k\|_{W'}^2).$$

Hence, (4.4.5) can be written as

$$\|E^k\|_{W'}^2 + \|B^{k+\frac{1}{2}}\|_W^2 \le \frac{1+\delta}{1-\delta}(\|E^0\|_{W'}^2 + \|B^{\frac{1}{2}}\|_W^2) + \frac{1}{1-\delta}\sum_{n=0}^{k-1} R^{n+\frac{1}{2}}. \tag{4.4.6}$$

Now, using Cauchy Schwarz inequality and the definitions of W'-norm and $R^{n+\frac{1}{2}}$,

$$\sum_{n=0}^{k-1} R^{n+\frac{1}{2}} \le \frac{1-\delta}{2}\max_{0\le n\le k}\|E^n\|_{W'}^2 + \frac{2}{1-\delta}(\sum_{n=0}^{k-1}\|S^{'-1}\tilde{J}^{n+\frac{1}{2}}\|_{W'})^2. \tag{4.4.7}$$

Now, the desire estimate (4.4.4) follows from (4.4.6), (4.4.7) and the following inequality

$$(\sum_{n=0}^{k-1} \|S^{'-1}\tilde{J}^{n+\frac{1}{2}}\|_{W'})^2 \leq \frac{T}{\Delta t}\sum_{n=0}^{k-1} \|S^{'-1}\tilde{J}^{n+\frac{1}{2}}\|_{W'}^2 \leq T\int_0^T \|S^{'-1}\tilde{J}(t)\|_{W'}^2\, dt.$$

□

It is now in a position to study the convergence theory of the method (4.4.1)-(4.4.2). To do so, for brevity, we define

$$\mathbf{e}(E)^n := E^n - E_e(t_n) \quad , \quad \mathbf{e}(B)^n := B^n - B'_e(t_n), \tag{4.4.8}$$

$$\mathbf{f}(E)^n := E^n - E'_f(t_n) \quad , \quad \mathbf{f}(B)^n := B^n - B_f(t_n). \tag{4.4.9}$$

Then, we subtract (4.4.1) by (3.3.4) and (4.4.2) by (3.3.3) to obtain

$$S'(\mathbf{f}(E)^{n+1} - \mathbf{f}(E)^n) - \Delta t C'\mathbf{e}(B)^{n+\frac{1}{2}} = P_1^{n+\frac{1}{2}}, \tag{4.4.10}$$

$$S(\mathbf{f}(B)^{n+\frac{3}{2}} - \mathbf{f}(B)^{n+\frac{1}{2}}) + \Delta t C\mathbf{e}(E)^{n+1} = P_2^{n+1}, \tag{4.4.11}$$

where

$$P_1^{n+\frac{1}{2}} := \tilde{J}^{n+\frac{1}{2}} - S'(E'_f(t_{n+1}) - E'_f(t_n)) + \Delta t C' B'_e(t_{n+\frac{1}{2}}), \tag{4.4.12}$$

$$P_2^{n+1} := -S(B_f(t_{n+\frac{3}{2}}) - B_f(t_{n+\frac{1}{2}})) - \Delta t C E_e(t_{n+1}). \tag{4.4.13}$$

Multiplying (4.4.10) by $D\mathbf{e}(E)^n + D\mathbf{e}(E)^{n+1}$ and (4.4.11) by $D'\mathbf{e}(B)^{n+\frac{3}{2}} + D'\mathbf{e}(B)^{n+\frac{1}{2}}$ and adding the two resulting equations,

$$\begin{aligned}
&(\mathbf{f}(E)^{n+1} - \mathbf{f}(E)^n, \mathbf{e}(E)^n + \mathbf{e}(E)^{n+1})_{W'} \\
&+ (\mathbf{f}(B)^{n+\frac{3}{2}} - \mathbf{f}(B)^{n+\frac{1}{2}}, \mathbf{e}(B)^{n+\frac{3}{2}} + \mathbf{e}(B)^{n+\frac{1}{2}})_W \\
=\ &(P_1^{n+\frac{1}{2}}, D(\mathbf{e}(E)^n + \mathbf{e}(E)^{n+1})) + (P_2^{n+1}, D'(\mathbf{e}(B)^{n+\frac{3}{2}} + \mathbf{e}(B)^{n+\frac{1}{2}})) \\
&+ \Delta t(C'\mathbf{e}(B)^{n+\frac{1}{2}}, D(\mathbf{e}(E)^n + \mathbf{e}(E)^{n+1})) \\
&- \Delta t(C\mathbf{e}(E)^{n+1}, D'(\mathbf{e}(B)^{n+\frac{3}{2}} + \mathbf{e}(B)^{n+\frac{1}{2}})).
\end{aligned} \tag{4.4.14}$$

By (2.2.7), (4.4.8) and (4.4.9), we obtain from (4.4.14) the following

$$\begin{aligned}
&(\mathbf{e}(E)^{n+1} - \mathbf{e}(E)^n, \mathbf{e}(E)^n + \mathbf{e}(E)^{n+1})_{W'} \\
&+ (\mathbf{e}(B)^{n+\frac{3}{2}} - \mathbf{e}(B)^{n+\frac{1}{2}}, \mathbf{e}(B)^n + \mathbf{e}(B)^{n+1})_W \\
=\ &((E'_f(t_{n+1}) - E_e(t_{n+1})) - (E'_f(t_n) - E_e(t_n)), \mathbf{e}(E)^n + \mathbf{e}(E)^{n+1})_{W'} \\
&+ ((B'_f(t_{n+\frac{3}{2}}) - B_e(t_{n+\frac{3}{2}})) - (B'_f(t_{n+\frac{1}{2}}) - B_e(t_{n+\frac{1}{2}})), \mathbf{e}(B)^{n+\frac{3}{2}} + \mathbf{e}(B)^{n+\frac{1}{2}})_W \\
&+ (P_1^{n+\frac{1}{2}}, D(\mathbf{e}(E)^n + \mathbf{e}(E)^{n+1})) + (P_2^{n+1}, D'(\mathbf{e}(B)^{n+\frac{3}{2}} + \mathbf{e}(B)^{n+\frac{1}{2}})) \\
&+ \Delta t(C'\mathbf{e}(B)^{n+\frac{1}{2}}, D\mathbf{e}(E)^n) - \Delta t(D\mathbf{e}(E)^{n+1}, C'\mathbf{e}(B)^{n+\frac{3}{2}}).
\end{aligned}$$

Adding from $n = 0$ to $n = k-1$, we have

$$
\begin{aligned}
&\|\mathbf{e}(E)^k\|_{W'}^2 + \|\mathbf{e}(B)^{k+\frac{1}{2}}\|_W^2 \\
= & -\Delta t(D\mathbf{e}(E)^k, C'\mathbf{e}(B)^{k+\frac{1}{2}}) \\
& + \sum_{n=0}^{k-1} \big\{((E_f'(t_{n+1}) - E_e(t_{n+1})) - (E_f'(t_n) - E_e(t_n)), \mathbf{e}(E)^n + \mathbf{e}(E)^{n+1})_{W'} \\
& + ((B_f(t_{n+\frac{3}{2}}) - B_e'(t_{n+\frac{3}{2}})) - (B_f(t_{n+\frac{1}{2}}) - B_e'(t_{n+\frac{1}{2}})), \mathbf{e}(B)^{n+\frac{1}{2}} + \mathbf{e}(B)^{n+\frac{3}{2}})_W \\
& + (P_1^{n+\frac{1}{2}}, D(\mathbf{e}(E)^n + \mathbf{e}(E)^{n+1})) + (P_2^{n+1}, D'(\mathbf{e}(B)^{n+\frac{1}{2}} + \mathbf{e}(B)^{n+\frac{3}{2}}))\big\}.
\end{aligned}
\tag{4.4.15}
$$

Before stating the result on error estimate of the explicit fully discrete scheme (4.4.1)-(4.4.2), we need the following two technical lemmas. The proof can be found in Theorem 5.1 of [5].

LEMMA 4.2. *Assume* $(\dot{\mathbf{B}}, \dot{\mathbf{E}}) \in (W^{1,p}(\Omega_r)^3)^2$ *for* $r = 1, 2$ *and* $p > 2$. *Then*

$$\|\dot{B}_f - \dot{B}_e'\|_W \leq Kh \sum_{r=1}^{2} |\mu_r^{-\frac{1}{2}} \dot{\mathbf{B}}|_{W^{1,p}(\Omega_r)^3}, \tag{4.4.16}$$

$$\|\dot{E}_f' - \dot{E}_e\|_{W'} \leq Kh \sum_{r=1}^{2} |\varepsilon_r^{\frac{1}{2}} \dot{\mathbf{E}}|_{W^{1,p}(\Omega_r)^3}, \tag{4.4.17}$$

where the constant K *is independent of mesh size and material coefficients* μ *and* ε.

In this paper, we will use the dot to represent time derivatives. The second one is the truncation error for the discretization of the semi-discrete scheme (3.3.5)-(3.3.6) by leap-frog time stepping.

LEMMA 4.3. *Assume* $(\mathbf{B}, \mathbf{E}) \in H^2(0, T; W^{1,p}(\Omega_r)^3)^2$ *for* $p > 2$ *and* $r = 1, 2$. *Then for general unstructured grids,*

$$\sum_{n=0}^{k-1} \|S'^{-1} P_1^{n+\frac{1}{2}}\|_{W'} \leq c_m K (\Delta t)^2 \sum_{r=1}^{2} \|\mu_r^{-\frac{1}{2}} \mathbf{B}\|_{H^2(0,T;W^{1,p}(\Omega_r)^3)}, \tag{4.4.18}$$

$$\sum_{n=0}^{k-1} \|S^{-1} P_2^{n+1}\|_W \leq c_m K (\Delta t)^2 \sum_{r=1}^{2} \|\varepsilon_r^{\frac{1}{2}} \mathbf{E}\|_{H^2(0,T;W^{1,p}(\Omega_r)^3)}. \tag{4.4.19}$$

Proof. We will give a proof for (4.4.18). The proof for (4.4.19) can be done in a similiar way. For the jth dual face, using (3.3.4) and (4.4.12), we have

$$(P_1^{n+\frac{1}{2}})_j = -\int_{n\Delta t}^{(n+1)\Delta t} (C'B_e')_j(s)\, ds + \Delta t (C'B_e')_j(t_{n+\frac{1}{2}}).$$

By the Sobolev embedding theorem, $H^2(n\Delta t, (n+1)\Delta t) \hookrightarrow C^1(n\Delta t, (n+1)\Delta t)$. Thus, $(P_1^{n+\frac{1}{2}})_j$ defines a bounded linear functional on $W^{2,1}(n\Delta t, (n+1)\Delta t)$ and vanishes for any linear functions in time. So by the Bramble-Hilbert lemma,

$$|(P_1^{n+\frac{1}{2}})_j| \leq K_1 \int_{n\Delta t}^{(n+1)\Delta t} |(C'\ddot{B}_e')_j(s)|\, ds,$$

where K_1 is a constant depending only on Δt. By using a standard scale change technique, we have

$$|(P_1^{n+\frac{1}{2}})_j| \le K(\Delta t)^2 \int_{n\Delta t}^{(n+1)\Delta t} |(C'\ddot{B}_e')_j(s)|\, ds.$$

Notice that for any non-interface dual face κ_j', we have

$$(C'\ddot{B}_e')_j = \int_{\kappa_j'} (\mathbf{curl}\,\ddot{\mathbf{H}}) \cdot \mathbf{n}\, d\sigma,$$

while for any interface dual face κ_j', we have

$$(C'\ddot{B}_e')_j = \int_{\partial\kappa_j'} \ddot{\mathbf{H}} \cdot \mathbf{t}\, dl = \sum_{r=1}^{2} \int_{\kappa_j' \cap \Omega_r} (\mathbf{curl}\,\ddot{\mathbf{H}}) \cdot \mathbf{n}\, d\sigma,$$

where the last equality follows from the tangential continuity of $\mathbf{H}$ across the interface Γ (see (1.1.8)). Thus, the term $(C'\ddot{B}_e)_j$ vanishes for constant functions in space. By the Sobolev embedding theorem, $W^{1,p}(\tau_i') \hookrightarrow L^1(\sigma_k')$ for $p > 2$. So, $(C'\ddot{B}_e')_j$ defines a bounded linear functional on $W^{1,p}(\tau_k' \cup \tau_l')^3$ and by the Bramble-Hilbert lemma,

$$|(C'\ddot{B}_e')_j| \le K_2 |\ddot{\mathbf{H}}|_{W^{1,p}(\tau_k' \cup \tau_l')^3}$$

where τ_k' and τ_l' are two dual elements sharing the same dual face κ_j', K_2 is a constant depending only on h. The standard scale change argument yields

$$|(C'\ddot{B}_e')_j| \le K h^{2-\frac{3}{p}} |\ddot{\mathbf{H}}|_{W^{1,p}(\tau_k' \cup \tau_l')^3}.$$

So, we have

$$|(P_1^{n+\frac{1}{2}})_j| \le K h^{2-\frac{3}{p}} (\Delta t)^2 \int_{n\Delta t}^{(n+1)\Delta t} |\ddot{\mathbf{H}}|_{W^{1,p}(\tau_k' \cup \tau_l')^3}\, ds.$$

By (1.1.9) and the definitions of c_m and W'-norm,

$$\|S'^{-1} P_1^{n+\frac{1}{2}}\|_{W'} \le c_m K (\Delta t)^{\frac{5}{2}} \sum_{r=1}^{2} \|\mu_r^{-\frac{1}{2}} \ddot{\mathbf{B}}\|_{L^2(n\Delta t,(n+1)\Delta t; W^{1,p}(\Omega_r)^3)}.$$

and consequently,

$$\sum_{n=0}^{k-1} \|S'^{-1} P_1^{n+\frac{1}{2}}\|_{W'} \le c_m K (\Delta t)^2 \sum_{r=1}^{2} \|\mu_r^{-\frac{1}{2}} \ddot{\mathbf{B}}\|_{L^2(0,T; W^{1,p}(\Omega_r)^3)}.$$

□

The following theorem gives the main result of this section. It states that the explicit scheme (4.4.1)-(4.4.2) is first order convergent in space and second order convergent in time under an assumption on the regularity of the true solution and a CFL stability condition.

THEOREM 4.4. *Assume that* $(\mathbf{E},\mathbf{B}) \in H^2(0,T;W^{1,p}(\Omega_r)^3)^2$, $p>2$, $r=1,2$, *is the solution to (1.1.1)-(1.1.2) and* $(E^n, B^{n+\frac{1}{2}})$ *is the solution to the explicit fully discrete scheme (4.4.1)-(4.4.2). Then, under the stability condition (4.4.3),*

$$\max_{0\le n\le N_T-1}(\|E^n - E_e(t_n)\|_{W'} + \|B^{n+\frac{1}{2}} - B_e'(t_{n+\frac{1}{2}})\|_W) \le \frac{K}{\sqrt{1-\delta}}(h + c_m(\Delta t)^2)\sum_{r=1}^{2}\|(\varepsilon_r^{\frac{1}{2}}\mathbf{E}, \mu_r^{-\frac{1}{2}}\mathbf{B})\|_{H^2(0,T;W^{1,p}(\Omega_r)^3)^2}. \tag{4.4.20}$$

Proof. The proof is based on (4.4.15). First, by resembling the techniques used in the proof of Theorem 4.1, we have

$$\Delta t(D\mathbf{e}(E)^k, C'\mathbf{e}(B)^{k+\frac{1}{2}}) \le \Delta t c_m \frac{M_2^{\frac{3}{2}}M_3^{\frac{1}{2}}}{\min(h)}(\|\mathbf{e}(B)^{k+\frac{1}{2}}\|_W^2 + \|\mathbf{e}(E)^k\|_{W'}^2).$$

Secondly, by integrating in time and the definition of W'-norm, we have

$$\|(E_f'(t_{n+1}) - E_e(t_{n+1})) - (E_f'(t_n) - E_e(t_n))\|_{W'}^2 \le \Delta t \int_{n\Delta t}^{(n+1)\Delta t} \|\dot{E}_f' - \dot{E}_e\|_{W'}^2\, ds.$$

Using (4.4.17),

$$\|(E_f'(t_{n+1}) - E_e(t_{n+1})) - (E_f'(t_n) - E_e(t_n))\|_{W'} \le Kh\sqrt{\Delta t}\sum_{r=1}^{2}\|\varepsilon_r^{\frac{1}{2}}\dot{\mathbf{E}}\|_{L^2(n\Delta t,(n+1)\Delta t;W^{1,p}(\Omega_r)^3)}. \tag{4.4.21}$$

So,

$$((E_f'(t_{n+1}) - E_e(t_{n+1})) - (E_f'(t_n) - E_e(t_n)), \mathbf{e}(E)^n + \mathbf{e}(E)^{n+1})_{W'} \le Kh\sqrt{\Delta t}\max_{0\le n\le k}\|\mathbf{e}(E)^n\|_{W'}\sum_{r=1}^{2}\|\varepsilon_r^{\frac{1}{2}}\dot{\mathbf{E}}\|_{L^2(n\Delta t,(n+1)\Delta t;W^{1,p}(\Omega_r)^3)}.$$

Similiarly, by using (4.4.16), we have

$$((B_f(t_{n+\frac{3}{2}}) - B_e'(t_{n+\frac{3}{2}}) - (B_f(t_{n+\frac{1}{2}}) - B_e'(t_{n+\frac{1}{2}})), \mathbf{e}(B)^{n+\frac{1}{2}} + \mathbf{e}(B)^{n+\frac{3}{2}})_W \le Kh\sqrt{\Delta t}\max_{0\le n\le k}\|\mathbf{e}(B)^{n+\frac{1}{2}}\|_W\sum_{r=1}^{2}\|\mu_r^{\frac{1}{2}}\dot{\mathbf{B}}\|_{L^2((n+\frac{1}{2})\Delta t,(n+\frac{3}{2})\Delta t;W^{1,p}(\Omega_r)^3)}.$$

Thirdly, by Cauchy Schwarz inequality,

$$(P_1^{n+\frac{1}{2}}, D(\mathbf{e}(E)^n + \mathbf{e}(E)^{n+1})) \le \|S^{'-1}P_1^{n+\frac{1}{2}}\|_{W'}\|\mathbf{e}(E)^n + \mathbf{e}(E)^{n+1}\|_{W'}$$
$$(P_2^{n+1}, D'(\mathbf{e}(B)^{n+\frac{1}{2}} + \mathbf{e}(B)^{n+\frac{3}{2}})) \le \|S^{-1}P_2^{n+1}\|_W\|\mathbf{e}(B)^{n+\frac{1}{2}} + \mathbf{e}(B)^{n+\frac{3}{2}}\|_W.$$

By (4.4.18), we have

$$\sum_{n=0}^{k-1}(P_1^{n+\frac{1}{2}}, D(\mathbf{e}(E)^n + \mathbf{e}(E)^{n+1})) \le c_m K(\Delta t)^2\max_{0\le n\le k}\|\mathbf{e}(E)^n\|_{W'}\sum_{r=1}^{2}\|\mu_r^{-\frac{1}{2}}\mathbf{B}\|_{H^2(0,T;W^{1,p}(\Omega_r)^3)}.$$

Similiarly, by (4.4.19), we have

$$\sum_{n=0}^{k-1}(P_2^{n+1}, D'(\mathbf{e}(B)^{n+\frac{1}{2}} + \mathbf{e}(B)^{n+\frac{3}{2}}))$$

$$\leq c_m K(\Delta t)^2 \max_{0\leq n\leq k} \|\mathbf{e}(B)^{n+\frac{1}{2}}\|_W \sum_{r=1}^{2} \|\varepsilon_r^{\frac{1}{2}}\mathbf{E}\|_{H^2(0,T;W^{1,p}(\Omega_r)^3)}.$$

Now, by collecting all of the above results, we have shown the desired convergence estimate.

□

4.2. Implicit scheme. In this section, we will consider an implicit scheme for (3.3.5)-(3.3.6). We will apply a standard Crank-Nicolson time discretization. The approximate solutions of $\mathbf{E}(t)$ and $\mathbf{B}(t)$ will be obtained at t_n and denoted by E^n and B^n respectively. Given (E^n, B^n), the next approximation (E^{n+1}, B^{n+1}) will be obtained by solving

$$S'(E^{n+1} - E^n) - \frac{\Delta t}{2}(C'B^n + C'B^{n+1}) = \tilde{J}^{n+\frac{1}{2}}, \tag{4.4.22}$$

$$S(B^{n+1} - B^n) + \frac{\Delta t}{2}(CE^n + CE^{n+1}) = 0. \tag{4.4.23}$$

That is, in each time step, we need to solve a linear system $Ax = b$ for x with

$$A := \begin{pmatrix} S' & -\frac{\Delta t}{2}C' \\ \frac{\Delta t}{2}C & S \end{pmatrix} \quad \text{and} \quad b := \begin{pmatrix} \tilde{J}^{n+\frac{1}{2}} + S'E^n + \frac{\Delta t}{2}C'B^n \\ SB^n - \frac{\Delta t}{2}CE^n \end{pmatrix} \tag{4.4.24}$$

The question of well-posedness of the problem (4.4.22)-(4.4.23) will be given by the following theorem.

THEOREM 4.5. *The implicit fully discrete scheme (4.4.22)-(4.4.23) is well-posed. Moreover, the following stability inequality holds for* $1 \leq n \leq N_T$*:*

$$\|E^n\|_{W'}^2 + \|B^n\|_W^2 \leq 2\|E^0\|_{W'}^2 + 2\|B^0\|_W^2 + 4T\int_0^T \|S'^{-1}\tilde{J}(t)\|_{W'}^2 \, dt.$$

Proof. We first show the system (4.4.22)-(4.4.23) has a unique solution. To do this, we prove all eigenvalues of the matrix A in (4.4.24) are non-zero. We rewrite A as

$$A = \begin{pmatrix} S' & 0 \\ 0 & S \end{pmatrix} + \frac{\Delta t}{2}\begin{pmatrix} 0 & -C' \\ C & 0 \end{pmatrix}.$$

By the definitions of C and C', it suffices to consider the following matrix

$$A_1 := \begin{pmatrix} 0 & -G^T \\ G & 0 \end{pmatrix}.$$

Notice that

$$(A_1)^2 = \begin{pmatrix} -G^TG & 0 \\ 0 & -GG^T \end{pmatrix}.$$

So, $(A_1)^2$ is negative semi-definite which implies all eigenvalues of $(A_1)^2$ are non-positive. Consequently, all eigenvalues of A_1 are purely imaginary. Hence, from the definition of A, we know that all eigenvalues of A have positive real parts, which implies A is invertible.

To prove the stability estimate, we multiply (4.4.22) by $D(E^{n+1}+E^n)$ and (4.4.23) by $D'(B^{n+1}+B^n)$ and add up the two resulting equations using (2.2.7) to get

$$\begin{aligned}&(E^{n+1}-E^n, E^{n+1}+E^n)_{W'}+(B^{n+1}-B^n, B^{n+1}+B^n)_W\\ &=(\tilde{J}^{n+\frac{1}{2}}, D(E^{n+1}+E^n)),\end{aligned} \tag{4.4.25}$$

and conequently,

$$\|E^{n+1}\|^2_{W'}+\|B^{n+1}\|^2_W=\|E^n\|^2_{W'}+\|B^n\|^2_W+(\tilde{J}^{n+\frac{1}{2}}, D(E^{n+1}+E^n)).$$

By induction, we have, for any $0\le n\le N_T$,

$$\|E^n\|^2_{W'}+\|B^n\|^2_W=\|E^0\|^2_{W'}+\|B^0\|^2_W+\sum_{k=1}^n(\tilde{J}^{k-\frac{1}{2}}, D(E^k+E^{k-1})).$$

By Cauchy Schwarz inequality,

$$\sum_{k=1}^n(\tilde{J}^{k-\frac{1}{2}}, D(E^k+E^{k-1}))\le\frac{1}{2}\max_{0\le n\le N_T}\|E^k\|^2_{W'}+2(\sum_{k=1}^n\|S^{'-1}\tilde{J}^{k-\frac{1}{2}}\|_{W'})^2.$$

Now the desired estimate follows from

$$(\sum_{k=1}^n\|S^{'-1}\tilde{J}^{k-\frac{1}{2}}\|_{W'})^2\le\frac{T}{\Delta t}\sum_{k=1}^n\|S^{'-1}\tilde{J}^{k-\frac{1}{2}}\|^2_{W'}\le T\int_0^T\|S^{'-1}\tilde{J}(t)\|^2_{W'}\,dt.$$

□

It is now in a position to study the convergence theory of the method (4.4.22)-(4.4.23). To do so, we subtract (4.4.22) by (3.3.4) and (4.4.23) by (3.3.3) to obtain

$$S'(\mathbf{f}(E)^{n+1}-\mathbf{f}(E)^n)-\frac{\Delta t}{2}(C'\mathbf{e}(B)^n+C'\mathbf{e}(B)^{n+1})=Q_1^{n+\frac{1}{2}}, \tag{4.4.26}$$

$$S(\mathbf{f}(B)^{n+1}-\mathbf{f}(B)^n)+\frac{\Delta t}{2}(C\mathbf{e}(E)^n+C\mathbf{e}(E)^{n+1})=Q_2^{n+\frac{1}{2}}, \tag{4.4.27}$$

where

$$Q_1^{n+\frac{1}{2}}:=\tilde{J}^{n+\frac{1}{2}}-S'(E_f'(t_{n+1})-E_f'(t_n))+\frac{\Delta t}{2}(C'B_e'(t_n)+C'B_e'(t_{n+1})), \tag{4.4.28}$$

$$Q_2^{n+\frac{1}{2}}:=-S(B_f(t_{n+1})-B_f(t_n))-\frac{\Delta t}{2}(CE_e(t_n)+CE_e(t_{n+1})). \tag{4.4.29}$$

Multiplying (4.4.26) by $D\mathbf{e}(E)^n+D\mathbf{e}(E)^{n+1}$ and (4.4.27) by $D'\mathbf{e}(B)^n+D'\mathbf{e}(B)^{n+1}$ and adding the two resulting equations with (2.2.7),

$$\begin{aligned}&(\mathbf{f}(E)^{n+1}-\mathbf{f}(E)^n, \mathbf{e}(E)^n+\mathbf{e}(E)^{n+1})_{W'}+(\mathbf{f}(B)^{n+1}-\mathbf{f}(B)^n, \mathbf{e}(B)^n+\mathbf{e}(B)^{n+1})_W\\ &=(Q_1^{n+\frac{1}{2}}, D(\mathbf{e}(E)^n+\mathbf{e}(E)^{n+1}))+(Q_2^{n+\frac{1}{2}}, D'(\mathbf{e}(B)^n+\mathbf{e}(B)^{n+1})).\end{aligned}$$

So, we obtain

$$
\begin{aligned}
&(\mathbf{e}(E)^{n+1}-\mathbf{e}(E)^n, \mathbf{e}(E)^n+\mathbf{e}(E)^{n+1})_{W'} + (\mathbf{e}(B)^{n+1}-\mathbf{e}(B)^n, \mathbf{e}(B)^n+\mathbf{e}(B)^{n+1})_{W} \\
&= ((E_f'(t_{n+1})-E_e(t_{n+1})) - (E_f'(t_n)-E_e(t_n)), \mathbf{e}(E)^n+\mathbf{e}(E)^{n+1})_{W'} \\
&\quad + ((B_f'(t_{n+1})-B_e(t_{n+1})) - (B_f'(t_n)-B_e(t_n)), \mathbf{e}(B)^n+\mathbf{e}(B)^{n+1})_{W} \\
&\quad + (Q_1^{n+\frac{1}{2}}, D(\mathbf{e}(E)^n+\mathbf{e}(E)^{n+1})) + (Q_2^{n+\frac{1}{2}}, D'(\mathbf{e}(B)^n+\mathbf{e}(B)^{n+1})).
\end{aligned}
$$

Adding from $n=0$ to $n=k-1$, we have

$$
\begin{aligned}
&\|\mathbf{e}(E)^k\|_{W'}^2 + \|\mathbf{e}(B)^k\|_W^2 \\
&= \sum_{n=0}^{k-1} \{((E_f'(t_{n+1})-E_e(t_{n+1})) - (E_f'(t_n)-E_e(t_n)), \mathbf{e}(E)^n+\mathbf{e}(E)^{n+1})_{W'} \\
&\quad + ((B_f'(t_{n+1})-B_e(t_{n+1})) - (B_f'(t_n)-B_e(t_n)), \mathbf{e}(B)^n+\mathbf{e}(B)^{n+1})_{W} \\
&\quad + (Q_1^{n+\frac{1}{2}}, D(\mathbf{e}(E)^n+\mathbf{e}(E)^{n+1})) + (Q_2^{n+\frac{1}{2}}, D'(\mathbf{e}(B)^n+\mathbf{e}(B)^{n+1}))\}.
\end{aligned}
\tag{4.4.30}
$$

Similiar to Lemma 4.3, we have the following consistency error estimate of the Crank-Nicolson time discretization of (4.4.22)-(4.4.23).

LEMMA 4.6. *Assume that* $(\mathbf{B},\mathbf{E}) \in H^2(0,T;W^{1,p}(\Omega_r)^3)^2$ *for* $p>2$ *and* $r=1,2$. *Then on general unstructured grids,*

$$
\sum_{n=0}^{k-1} \|S'^{-1} Q_1^{n+\frac{1}{2}}\|_{W'} \le c_m K(\Delta t)^2 \sum_{r=1}^{2} \|\varepsilon_r^{\frac{1}{2}} \mathbf{E}\|_{H^2(0,T;W^{1,p}(\Omega_r)^3)}, \tag{4.4.31}
$$

$$
\sum_{n=0}^{k-1} \|S^{-1} Q_2^{n+\frac{1}{2}}\|_{W} \le c_m K(\Delta t)^2 \sum_{r=1}^{2} \|\mu_r^{-\frac{1}{2}} \mathbf{B}\|_{H^2(0,T;W^{1,p}(\Omega_r)^3)}. \tag{4.4.32}
$$

Proof. We will give the key idea for the proof of (4.4.31). By the definition of $Q_1^{n+\frac{1}{2}}$, for any dual face κ_j',

$$
(Q_1^{n+\frac{1}{2}})_j = -\int_{n\Delta t}^{(n+1)\Delta t} (C'B_e')_j(s)\, ds + \frac{\Delta t}{2}((C'B_e')_j(t_n) + (C'B_e')_j(t_{n+1})).
$$

Clearly, $(Q_1^{n+\frac{1}{2}})_j$ defines a bounded linear functional on $H^2(n\Delta t,(n+1)\Delta t)$ and vanishes for any linear functions in time. The Bramble-Hilbert lemma and scale change technique yield,

$$
|(Q_1^{n+\frac{1}{2}})_j| \le K(\Delta t)^2 \int_{n\Delta t}^{(n+1)\Delta t} (C'\ddot{B}_e')_j(s)\, ds.
$$

Now the same argument as in the proof of Lemma 4.3 can be applied to show the desire estimate.

□

The following theorem gives the main result in this section.

THEOREM 4.7. *Assume that* $(\mathbf{E},\mathbf{B}) \in H^2(0,T;W^{1,p}(\Omega_r)^3)^2$, $p>2$, $r=1,2$, *is the solution to (1.1.1)-(1.1.2) and* (E^n,B^n) *is the solution to the implicit fully discrete* *scheme (4.4.22)-(4.4.23). Then*

$$\begin{aligned}&\max_{0\le n\le N_T}(\|E^n-E_e(t_n)\|_{W'}+\|B^n-B_e'(t_n)\|_W)\\ \le&K(h+c_m(\Delta t)^2)\sum_{r=1}^{2}\|(\varepsilon_r^{\frac12}\mathbf{E},\mu_r^{-\frac12}\mathbf{B})\|_{H^2(0,T;W^{1,p}(\Omega_r)^3)^2}.\end{aligned}\tag{4.4.33}$$

Proof. The proof of this theorem is similar to that of Theorem 4.4 and is based on (4.4.30). First of all, the two terms

$$\begin{aligned}&(E_f'(t_{n+1})-E_e(t_{n+1}))-(E_f'(t_n)-E_e(t_n))\\&(B_f(t_{n+1})-B_e'(t_{n+1}))-(B_f(t_n)-B_e'(t_n))\end{aligned}$$

can be estimated in a way similiar to the proof of (4.4.21). The terms involving $Q_1^{n+\frac12}$ and $Q_2^{n+\frac12}$ can be estimated by using Lemma 4.6.

□

5. Analysis on rectangular grid. In this section, we will consider the explicit finite volume scheme (4.4.1)-(4.4.2) and the implicit finite volume scheme (4.4.22)-(4.4.23) on rectangular grids. It is clear that all primal and dual elements are cuboids and all faces are rectangles. All definitions that we made in previous sections can be made in exactly the same way on non-uniform rectangular grids. For instances, $M_3=4$ for rectangular grids. It can be shown that the two schemes (4.4.1)-(4.4.2) and (4.4.22)-(4.4.23) are second order convergent in space. The second order convergence comes from the fact that the circumcenter of a cuboid is also its barycenter. In section 5.2, we give a one dimensional counter example to show that without taking the barycenter as dual node the scheme may reduce to first order.

5.1. Convergence analysis. First of all, we emphasis here that we can apply the same technique in proving Lemma 4.2 to obtain the same estimate for rectangular grids. However, since the grids we are considering are non-uniform and there are some restrictions near the interface, we cannot get second order estimate. The following two technical lemmas describe some representation of spatial consistency error. They are Lemma 5.2 and Lemma 5.3 taken from [5].

LEMMA 5.1. *There exist functions $u(t)$ and $\xi(t)\in\mathbb{R}^{F_1}$ such that all the non-interface components of $\xi(t)$ vanish and all components of u and ξ are bounded linear functionals of $\mathbf{B}$ and the following relation holds for all $\phi\in\mathbb{R}^M$ with $\phi|_{\partial\Omega}=0$:*

$$(C\phi,D'(B_f-B_e'))=(C\phi,D'u)+(C\phi,\xi).\tag{5.5.1}$$

Furthermore, the following estimates hold for $u(t)$ and $\xi(t)$:

$$\|u\|_W\le Kh^2\sum_{i=1}^{2}\|\mu_i^{-\frac12}\mathbf{B}\|_{H^3(\Omega_i)^3},\quad \|D^{'-1}\xi\|_W\le Kh^2\sum_{i=1}^{2}\|\mu_i^{-\frac12}\mathbf{B}\|_{H^3(\Omega_i)^3}.\tag{5.5.2}$$

LEMMA 5.2. *There exist functions $v(t)$ and $\lambda(t)\in\mathbb{R}^{M_1}$ and $w(t)\in\mathbb{R}^{F_1}$ such that all the non-interface components of $\lambda(t)$ vanish and all the components of v,w and λ are bounded linear functionals of $\mathbf{E}$, and the following relation holds for all $\phi\in\mathbb{R}^{M_1}$ with $\phi|_{\partial\Omega}=0$:*

$$(\dot{E}_f'-\dot{E}_e,\phi)_{W'}=(\dot{v},\phi)_{W'}+(D'\dot{w},C\phi)+(S^{'-1}\dot{\lambda},\phi)_{W'}.\tag{5.5.3}$$

Furthermore, we have the following estimates for $v(t)$, $\lambda(t)$ and $w(t)$ and $p>3$:

$$\|\dot{v}\|_{W'} \le Kh^2 \sum_{i=1}^{2} \|\varepsilon_i^{\frac{1}{2}} \dot{\mathbf{E}}\|_{H^3(\Omega_i)^3}, \quad \|\dot{w}\|_W \le Kh^2 \sum_{i=1}^{2} \|\varepsilon_i^{\frac{1}{2}} \dot{\mathbf{E}}\|_{W^{2,p}(\Omega_i)^3}, \tag{5.5.4}$$

$$\|S^{'-1}\dot{\lambda}\|_{W'} \le Kh^2 \sum_{i=1}^{2} \|\varepsilon_i^{\frac{1}{2}} \dot{\mathbf{E}}\|_{H^3(\Omega_i)^3}. \tag{5.5.5}$$

Now, we will consider convergence analysis on the explicit fully discrete scheme (4.4.1)-(4.4.2) for non-uniform rectangular grids. To begin, from (4.4.14), we see that

$$\begin{aligned}
&(\mathbf{e}(E)^{n+1} - \mathbf{e}(E)^n, \mathbf{e}(E)^{n+1} + \mathbf{e}(E)^n)_{W'} \\
&+ (\mathbf{f}(B)^{n+\frac{3}{2}} - \mathbf{f}(B)^{n+\frac{1}{2}}, \mathbf{f}(B)^{n+\frac{3}{2}} + \mathbf{f}(B)^{n+\frac{1}{2}})_W \\
= {}& ((E_f'(t_{n+1}) - E_e(t_{n+1})) - (E_f'(t_n) - E_e(t_n)), \mathbf{e}(E)^{n+1} + \mathbf{e}(E)^n)_{W'} \\
&- (\mathbf{f}(B)^{n+\frac{3}{2}} - \mathbf{f}(B)^{n+\frac{1}{2}}, (B_f(t_{n+\frac{3}{2}}) - B_e'(t_{n+\frac{3}{2}})) + (B_f(t_{n+\frac{1}{2}}) - B_e'(t_{n+\frac{1}{2}})))_W \\
&+ (P_1^{n+\frac{1}{2}}, D(\mathbf{e}(E)^n + \mathbf{e}(E)^{n+1})) + (P_2^{n+1}, D'(\mathbf{e}(B)^{n+\frac{3}{2}} + \mathbf{e}(B)^{n+\frac{1}{2}})) \\
&+ \Delta t(C'\mathbf{e}(B)^{n+\frac{1}{2}}, D\mathbf{e}(E)^n) - \Delta t(D\mathbf{e}(E)^{n+1}, C'\mathbf{e}(B)^{n+\frac{3}{2}}).
\end{aligned}$$

Adding from $n=0$ to $n=k-1$, we have

$$\begin{aligned}
&\|\mathbf{e}(E)^k\|_{W'}^2 + \|\mathbf{f}(B)^{k+\frac{1}{2}}\|_W^2 \\
= {}& -\Delta t(D\mathbf{e}(E)^k, C'\mathbf{e}(B)^{k+\frac{1}{2}}) \\
&+ \sum_{n=0}^{k-1} \Big\{ ((E_f'(t_{n+1}) - E_e(t_{n+1})) - (E_f'(t_n) - E_e(t_n)), \mathbf{e}(E)^n + \mathbf{e}(E)^{n+1})_{W'} \\
&- (\mathbf{f}(B)^{n+\frac{3}{2}} - \mathbf{f}(B)^{n+\frac{1}{2}}, (B_f(t_{n+\frac{3}{2}}) - B_e'(t_{n+\frac{3}{2}})) + (B_f(t_{n+\frac{1}{2}}) - B_e'(t_{n+\frac{1}{2}})))_W \\
&+ (P_1^{n+\frac{1}{2}}, D(\mathbf{e}(E)^n + \mathbf{e}(E)^{n+1})) + (P_2^{n+1}, D'(\mathbf{e}(B)^{n+\frac{1}{2}} + \mathbf{e}(B)^{n+\frac{3}{2}})) \Big\}.
\end{aligned} \tag{5.5.6}$$

The following theorem gives the convergence result for the explicit finite volume scheme (4.4.1)-(4.4.2) on non-uniform rectangular grids.

THEOREM 5.3. *Assume that*

$$\begin{aligned}
&\mathbf{B}(\mathbf{x}, t) \in H^1(0, T; H^3(\Omega_r)^3) \\
&\mathbf{E}(\mathbf{x}, t) \in H^1(0, T; H^3(\Omega_r)^3) \cap H^2(0, T; W^{2,p}(\Omega_r)^3),
\end{aligned}$$

for $p>3$ and $r=1,2$, is the solution to (1.1.1)-(1.1.2) and $(E^n, B^{n+\frac{1}{2}})$ is the solution to the explicit fully discrete scheme (4.4.1)-(4.4.2) on non-uniform rectangular grids. Then, under the stability condition $\delta < \frac{1}{2}$,

$$\begin{aligned}
&\max_{0 \le n \le N_T - 1} (\|E^n - E_e(t_n)\|_{W'} + \|B^{n+\frac{1}{2}} - B_f(t_{n+\frac{1}{2}})\|_W) \\
\le {}& \frac{K}{\sqrt{1-\delta}} (h^2 + c_m (\Delta t)^2) \\
&\times \sum_{r=1}^{2} \Big\{ \|(\varepsilon_r^{\frac{1}{2}} \mathbf{E}, \mu_r^{-\frac{1}{2}} \mathbf{B})\|_{H^1(0,T;H^3(\Omega_r)^3)} + \|\varepsilon_r^{\frac{1}{2}} \mathbf{E}\|_{H^2(0,T;W^{2,p}(\Omega_r)^3)} \Big\}.
\end{aligned} \tag{5.5.7}$$

Proof. The proof is based on (5.5.6).

(i) To begin, notice that the first term in the right hand side of (5.5.6) can be estimated as follows:

$$\begin{aligned}
&\Delta t(D\mathbf{e}(E)^k, C'\mathbf{e}(B)^{k+\frac{1}{2}}) \\
&= \Delta t(D\mathbf{e}(E)^k, C'\mathbf{f}(B)^{k+\frac{1}{2}}) + \Delta t(D\mathbf{e}(E)^k, C'(B_f(t_{k+\frac{1}{2}}) - B'_e(t_{k+\frac{1}{2}}))).
\end{aligned}$$

Applying the technique used in proving Theorem 4.1, we have

$$\Delta t(D\mathbf{e}(E)^k, C'\mathbf{f}(B)^{k+\frac{1}{2}}) \le \Delta t c_m \frac{M_2^{\frac{3}{2}} M_3^{\frac{1}{2}}}{\min(h)} (\|\mathbf{e}(E)^k\|_{W'}^2 + \|\mathbf{f}(B)^{k+\frac{1}{2}}\|_W^2).$$

Applying (2.2.7) and (5.5.1), we have

$$\begin{aligned}
&\Delta t(D\mathbf{e}(E)^k, C'(B_f(t_{k+\frac{1}{2}}) - B'_e(t_{k+\frac{1}{2}}))) \\
&= \Delta t(C\mathbf{e}(E)^k, D'(B_f(t_{k+\frac{1}{2}}) - B'_e(t_{k+\frac{1}{2}}))) \\
&= \Delta t(C\mathbf{e}(E)^k, D'u^{k+\frac{1}{2}}) + \Delta t(C\mathbf{e}(E)^k, \xi^{k+\frac{1}{2}}) \\
&= \Delta t(D\mathbf{e}(E)^k, C'u^{k+\frac{1}{2}}) + \Delta t(D\mathbf{e}(E)^k, C'D'^{-1}\xi^{k+\frac{1}{2}}),
\end{aligned}$$

where $u^{k+\frac{1}{2}}$ and $\xi^{k+\frac{1}{2}}$ satisfy (5.5.2). So, we obtain

$$\begin{aligned}
&\Delta t(D\mathbf{e}(E)^k, C'(B_f(t_{k+\frac{1}{2}}) - B'_e(t_{k+\frac{1}{2}}))) \\
&\le \Delta t c_m \frac{M_2^{\frac{3}{2}} M_3^{\frac{1}{2}}}{\min(h)} (2\|\mathbf{e}(E)^k\|_{W'}^2 + \|u^{k+\frac{1}{2}}\|_W^2 + \|D'^{-1}\xi^{k+\frac{1}{2}}\|_W^2).
\end{aligned}$$

(ii) By (5.5.3) with $\phi = \mathbf{e}(E)^n + \mathbf{e}(E)^{n+1}$, we have

$$\begin{aligned}
&(E'_f(t_n) - E_e(t_n), \mathbf{e}(E)^n + \mathbf{e}(E)^{n+1}) \\
&= (v^n, \mathbf{e}(E)^n + \mathbf{e}(E)^{n+1})_{W'} + (D'w^n, C(\mathbf{e}(E)^n + \mathbf{e}(E)^{n+1})) \\
&\quad + (S'^{-1}\lambda^n, \mathbf{e}(E)^n + \mathbf{e}(E)^{n+1})_{W'}.
\end{aligned}$$

So, we have

$$\begin{aligned}
&((E'_f(t_{n+1}) - E_e(t_{n+1})) - (E'_f(t_n) - E_e(t_n)), \mathbf{e}(E)^n + \mathbf{e}(E)^{n+1}) \\
&= \int_{n\Delta t}^{(n+1)\Delta t} \Big\{ (\dot{v}, \mathbf{e}(E)^n + \mathbf{e}(E)^{n+1})_{W'} + (D'\dot{w}, C(\mathbf{e}(E)^n + \mathbf{e}(E)^{n+1})) \\
&\quad + (S'^{-1}\dot{\lambda}, \mathbf{e}(E)^n + \mathbf{e}(E)^{n+1})_{W'} \Big\}\, ds \\
&\le 2(\max_{0\le n\le k} \|\mathbf{e}(E)^n\|_{W'}) \times \| \int_{n\Delta t}^{(n+1)\Delta t} (\dot{v} + S'^{-1}\dot{\lambda})\, ds\|_{W'} \\
&\quad + \int_{n\Delta t}^{(n+1)\Delta t} (D'\dot{w}, C(\mathbf{e}(E)^n + \mathbf{e}(E)^{n+1}))\, ds.
\end{aligned}$$

By the definition of W'-norm and (5.5.4),

$$\begin{aligned}
\| \int_{n\Delta t}^{(n+1)\Delta t} \dot{v}\, ds\|_{W'}^2 &\le \Delta t \int_{n\Delta t}^{(n+1)\Delta t} \|\dot{v}\|_{W'}^2\, ds \\
&\le K h^4 \Delta t \sum_{r=1}^{2} \|\varepsilon_r^{\frac{1}{2}} \dot{\mathbf{E}}\|_{L^2(n\Delta t,(n+1)\Delta t; H^3(\Omega_r)^3)}^2.
\end{aligned}$$

Similiarly, by the definition of W'-norm and (5.5.5), we have

$$\| \int_{n\Delta t}^{(n+1)\Delta t} S'^{-1}\dot{\lambda}\; ds\|_{W'}^2 \le Kh^4\Delta t \sum_{r=1}^{2} \|\varepsilon_r^{\frac{1}{2}}\dot{\mathbf{E}}\|^2_{L^2(n\Delta t,(n+1)\Delta t;H^3(\Omega_r)^3)}.$$

Using (4.4.11) and the mean value theorem for integral, we have

$$\begin{aligned}
&\int_{n\Delta t}^{(n+1)\Delta t} (D'\dot{w}, C(\mathbf{e}(E)^n + \mathbf{e}(E)^{n+1}))\; ds \\
=& -\frac{1}{\Delta t}\int_{n\Delta t}^{(n+1)\Delta t} \Big\{(D'\dot{w}, S(\mathbf{f}(B)^{n+\frac{3}{2}} - \mathbf{f}(B)^{n-\frac{1}{2}})) - (D'\dot{w}, P_2^n + P_2^{n+1})\Big\}\; ds \\
=& -(D'\dot{w}(\eta^{n+\frac{1}{2}}), S(\mathbf{f}(B)^{n+\frac{3}{2}} - \mathbf{f}(B)^{n-\frac{1}{2}})) + \frac{1}{\Delta t}\int_{n\Delta t}^{(n+1)\Delta t} (D'\dot{w}, P_2^n + P_2^{n+1})\; ds,
\end{aligned}$$

where $t_n < \eta^{n+\frac{1}{2}} < t_{n+1}$. Applying summation by parts,

$$\begin{aligned}
&\sum_{n=0}^{k-1}(D'\dot{w}(\eta^{n+\frac{1}{2}}), S(\mathbf{f}(B)^{n+\frac{3}{2}} - \mathbf{f}(B)^{n-\frac{1}{2}})) \\
=& (D'\dot{w}(\eta^{k-\frac{1}{2}}), S\mathbf{f}(B)^{k+\frac{1}{2}}) - \sum_{n=1}^{k-2}(D'(\dot{w}(\eta^{n+\frac{3}{2}}) - \dot{w}(\eta^{n-\frac{1}{2}})), S\mathbf{f}(B)^{n+\frac{1}{2}}).
\end{aligned}$$

Notice that

$$|\dot{w}(\eta^{n+\frac{3}{2}}) - \dot{w}(\eta^{n-\frac{1}{2}})|^2 \le 3\Delta t \int_{(n-1)\Delta t}^{(n+2)\Delta t} |\ddot{w}|^2\; ds.$$

By the definition of W-norm and the second estimate of (5.5.4),

$$\|\dot{w}(\eta^{n+\frac{3}{2}}) - \dot{w}(\eta^{n-\frac{1}{2}})\|_W^2 \le Kh^4\Delta t \sum_{r=1}^{2} \|\varepsilon_r^{\frac{1}{2}}\ddot{\mathbf{E}}\|^2_{L^2((n-1)\Delta t,(n+2)\Delta t;W^{2,p}(\Omega_r)^3)}.$$

By the Sobolev embedding theorem $H^2(0,T) \hookrightarrow C^1(0,T)$ and the second estimate of (5.5.4), we get

$$\begin{aligned}
&\frac{1}{\Delta t}\int_{n\Delta t}^{(n+1)\Delta t} (D'\dot{w}, P_2^n + P_2^{n+1})\; ds \\
\le& \max_{0\le s\le T} \|\dot{w}(s)\|_W \|S^{-1}(P_2^n + P_2^{n+1})\|_W \\
\le& Kh^2\|S^{-1}(P_2^n + P_2^{n+1})\|_W \sum_{r=1}^{2} \|\varepsilon_r^{\frac{1}{2}}\mathbf{E}\|_{H^2(0,T;W^{2,p}(\Omega_r)^3)}.
\end{aligned}$$

(iii) Using (4.4.11) and (4.4.13), we have

$$\begin{aligned}
&S(\mathbf{f}(B)^{n+\frac{3}{2}} - \mathbf{f}(B)^{n+\frac{1}{2}}) \\
=& -\Delta t C\mathbf{e}(E)^{n+1} + P_2^{n+1} \\
=& -\Delta t C\mathbf{e}(E)^{n+1} - \int_{(n+\frac{1}{2})\Delta t}^{(n+\frac{3}{2})\Delta t} S\dot{B}_f\; ds - \Delta t C E_e(t_{n+1}).
\end{aligned}$$

By (3.3.3), we have $S(\mathbf{f}(B)^{n+\frac{3}{2}} - \mathbf{f}(B)^{n+\frac{1}{2}}) = C\phi$ with

$$\phi = -\Delta t\mathbf{e}(E)^{n+1} + \int_{(n+\frac{1}{2})\Delta t}^{(n+\frac{3}{2})\Delta t} E_e(s)\, ds - E_e(t_{n+1}).$$

Hence, by (5.5.1), we have

$$\begin{aligned}&(\mathbf{f}(B)^{n+\frac{3}{2}} - \mathbf{f}(B)^{n+\frac{1}{2}}, B_f(t_{n+\frac{3}{2}}) - B_e'(t_{n+\frac{3}{2}})_W \\ &= (\mathbf{f}(B)^{n+\frac{3}{2}} - \mathbf{f}(B)^{n+\frac{1}{2}}, u^{n+\frac{3}{2}})_W + (\mathbf{f}(B)^{n+\frac{3}{2}} - \mathbf{f}(B)^{n+\frac{1}{2}}, D^{'-1}\xi^{n+\frac{3}{2}})_W.\end{aligned}$$

Applying summation by parts, we obtain

$$\begin{aligned}&\sum_{n=0}^{k-1} (\mathbf{f}(B)^{n+\frac{3}{2}} - \mathbf{f}(B)^{n+\frac{1}{2}}, u^{n+\frac{3}{2}})_W \\ &\quad = (\mathbf{f}(B)^{k+\frac{1}{2}}, u^{k+\frac{1}{2}})_W - \sum_{n=1}^{k-1}(\mathbf{f}(B)^{n+\frac{1}{2}}, u^{n+\frac{3}{2}} - u^{n+\frac{1}{2}})_W.\end{aligned}$$

We remark that a similiar result holds for $(\mathbf{f}(B)^{n+\frac{3}{2}} - \mathbf{f}(B)^{n+\frac{1}{2}}, D^{'-1}\xi^{n+\frac{3}{2}})_W$.

(iv) We have

$$(P_1^{n+\frac{1}{2}}, D(\mathbf{e}(E)^n + \mathbf{e}(E)^{n+1})) \leq \|S^{'-1}P_1^{n+\frac{1}{2}}\|_{W'}\|\mathbf{e}(E)^n + \mathbf{e}(E)^{n+1}\|_{W'}$$

which can be estimated by using (4.4.18).

(v) Notice that

$$\begin{aligned}&(P_2^{n+1}, D'(\mathbf{e}(B)^{n+\frac{1}{2}} + \mathbf{e}(B)^{n+\frac{3}{2}})) \\ &= (P_2^{n+1}, D'(\mathbf{f}(B)^{n+\frac{1}{2}} + \mathbf{f}(B)^{n+\frac{3}{2}})) \\ &\quad - (P_2^{n+1}, D'((B_f(t_{n+\frac{3}{2}}) - B_e'(t_{n+\frac{3}{2}})) + (B_f(t_{n+\frac{1}{2}}) - B_e'(t_{n+\frac{1}{2}}))).\end{aligned}$$

The first term on the right hand side can be estimated by using (4.4.19). Notice that P_2^{n+1} can be written as $C\tilde{\phi}$ for some $\tilde{\phi}$. So, by (5.5.1), we have

$$(P_2^{n+1}, D'(B_f(t_{n+\frac{3}{2}}) - B_e'(t_{n+\frac{3}{2}}))) = (P_2^{n+1}, D'u^{n+\frac{3}{2}}) + (P_2^{n+1}, \xi^{n+\frac{3}{2}}),$$

which can be estimated by using (4.4.19) and (5.5.2).

□

We are now in a position to analyse the convergence of the implicit fully discrete scheme (4.4.22)-(4.4.23) for non-uniform rectangular grids. To begin, from (4.4.25), we see that

$$\begin{aligned}&(\mathbf{e}(E)^{n+1} - \mathbf{e}(E)^n, \mathbf{e}(E)^{n+1} + \mathbf{e}(E)^n)_{W'} \\ &\quad + (\mathbf{f}(B)^{n+1} - \mathbf{f}(B)^n, \mathbf{f}(B)^{n+1} + \mathbf{f}(B)^n)_W \\ &= ((E_f'(t_{n+1}) - E_e(t_{n+1})) - (E_f'(t_n) - E_e(t_n)), \mathbf{e}(E)^{n+1} + \mathbf{e}(E)^n)_{W'} \\ &\quad - (\mathbf{f}(B)^{n+1} - \mathbf{f}(B)^n, (B_f(t_{n+1}) - B_e'(t_{n+1})) + (B_f(t_n) - B_e'(t_n)))_W \\ &\quad + (Q_1^{n+\frac{1}{2}}, D(\mathbf{e}(E)^n + \mathbf{e}(E)^{n+1})) + (Q_2^{n+\frac{1}{2}}, D'(\mathbf{e}(B)^{n+1} + \mathbf{e}(B)^n)).\end{aligned}$$

Adding from $n = 0$ to $n = k-1$, we have

$$
\begin{aligned}
&\|\mathbf{e}(E)^k\|_{W'}^2 + \|\mathbf{f}(B)^k\|_W^2 \\
&= + \sum_{n=0}^{k-1} \Big\{ ((E_f'(t_{n+1}) - E_e(t_{n+1})) - (E_f'(t_n) - E_e(t_n)), \mathbf{e}(E)^n + \mathbf{e}(E)^{n+1})_{W'} \\
&\quad - (\mathbf{f}(B)^{n+1} - \mathbf{f}(B)^n, (B_f(t_{n+1}) - B_e'(t_{n+1})) + (B_f(t_n) - B_e'(t_n)))_W \\
&\quad + (Q_1^{n+\frac{1}{2}}, D(\mathbf{e}(E)^n + \mathbf{e}(E)^{n+1})) + (Q_2^{n+\frac{1}{2}}, D'(\mathbf{e}(B)^n + \mathbf{e}(B)^{n+1})) \Big\}.
\end{aligned}
\tag{5.5.8}
$$

The following theorem gives the convergence result for the implicit finite volume scheme (4.4.22)-(4.4.23) on non-uniform rectangular grids.

THEOREM 5.4. *Assume that*

$$
\begin{aligned}
&\mathbf{B}(\mathbf{x}, t) \in H^1(0, T; H^3(\Omega_r)^3) \\
&\mathbf{E}(\mathbf{x}, t) \in H^1(0, T; H^3(\Omega_r)^3) \cap H^2(0, T; W^{2,p}(\Omega_r)^3),
\end{aligned}
$$

for $p > 3$ *and* $r = 1, 2$, *is the solution to (1.1.1)-(1.1.2) and* (E^n, B^n) *is the solution to the implicit fully discrete scheme (4.4.22)-(4.4.23) on non-uniform rectangular grids. Then,*

$$
\begin{aligned}
&\max_{0 \le n \le N_T} (\|E^n - E_e(t_n)\|_{W'} + \|B^n - B_f(t_n)\|_W) \\
&\le K(h^2 + c_m(\Delta t)^2) \\
&\quad \times \sum_{r=1}^{2} \Big\{ \|(\varepsilon_r^{\frac{1}{2}} \mathbf{E}, \mu_r^{-\frac{1}{2}} \mathbf{B})\|_{H^1(0,T;H^3(\Omega_r)^3)} + \|\varepsilon_r^{\frac{1}{2}} \mathbf{E}\|_{H^2(0,T;W^{2,p}(\Omega_r)^3)} \Big\}.
\end{aligned}
\tag{5.5.9}
$$

5.2. A counter example. We see from the previous sections that the spatial convergence of the finite volume method on rectangular grid is one order higher than that on general unstructured mesh. One main difference between these two grids is that the circumcenter of a rectangle coincides its barycenter. With chosing the barycenter as dual node, the scheme remains first order accurate. We will show this by considering the following one dimensional example. Consider the system

$$
\begin{aligned}
u_t &= v_x, \\
v_t &= u_x,
\end{aligned}
$$

with initial conditions

$$u(x, 0) = 0, \quad v(x, 0) = \frac{1}{2}x^2.$$

The exact solution to this problem is given by

$$u(x, t) = xt, \quad v(x, t) = \frac{1}{2}(x^2 + t^2).$$

Now, we consider a uniform grid with mesh size h. A dual node within each primal interval is chosen such that the distance between the left end point and the dual node is αh for fixed $0 < \alpha < 1$. Therefore, the distance between the right end point and the dual node is $(1-\alpha)h$. Also, the distance between two consecutive dual nodes is h. We consider the following semi-discrete scheme

$$\frac{d}{dt}u_j = \frac{v'_{j+1} - v'_j}{h},$$
$$\frac{d}{dt}v'_j = \frac{u_j - u_{j-1}}{h},$$

where u_j is defined corresponding to primal node x_j while v'_j is defined corresponding to dual node x'_j. By a direct computation, it can be shown that the following is a solution to the semi-discrete scheme

$$u_j = x_j t + (\alpha^2 - (1-\alpha)^2)ht,$$
$$v'_j = \frac{1}{2}((x'_j)^2 + t^2),$$

resulting in a $O(h)$ error.

6. Remarks on the relationship between finite volume and finite element methods. In this section, we will show that the linear edge finite element method, with some suitable choice of quadrature rules in the evaluations of mass and stiffness matrices, reduces to the finite volume method (3.3.5)-(3.3.6). To make the idea clearer, we will consider the spatial discretization only.

We formulate the problem as (see [14] [16]): find $(\mathbf{E}, \mathbf{H})$ such that

$$(\varepsilon \mathbf{E}_t, \phi) - (\mathbf{H}, \nabla \times \phi) = (\mathbf{J}, \phi), \quad \forall \phi \in H_0(\mathrm{curl}, \Omega), \tag{6.6.1}$$
$$(\mu \mathbf{H}_t, \psi) + (\nabla \times \mathbf{E}, \psi) = 0, \quad \forall \psi \in H(\mathrm{div}, \Omega). \tag{6.6.2}$$

Let $U_h \subset H_0(\mathrm{curl}, \Omega)$ and $V_h \subset H(\mathrm{div}, \Omega)$ be finite dimensional subspaces. Then, the Nédélec finite element method can be formulate as: find $(\mathbf{E}^h, \mathbf{H}^h)$ such that

$$(\varepsilon \mathbf{E}^h_t, \phi^h) - (\mathbf{H}^h, \nabla \times \phi^h) = (\mathbf{J}, \phi^h), \quad \forall \phi^h \in U_h, \tag{6.6.3}$$
$$(\mu \mathbf{H}^h_t, \psi^h) + (\nabla \times \mathbf{E}^h, \psi^h) = 0, \quad \forall \psi^h \in V_h. \tag{6.6.4}$$

We will consider U_h and V_h to be Nédélec linear curl- and div-conforming finite element spaces respectively.

6.1. Rectangular grids. In this section, We will show that, on rectangular grids, the finite element method (6.6.3)-(6.6.4) with evaluation of integrals by trapezoidal rule is the same as the semi-discrete finite volume method (3.3.5)-(3.3.6) with a different source term $\tilde{J}$. In this case, the degrees of freedom of U_h is given by the set

$$\Sigma^U(\mathbf{u}, \tau) = \{ \, (u_e)_j = \frac{1}{h_j} \int_{\sigma_j} \mathbf{u} \cdot \mathbf{t} \, dl, \ \forall \sigma_j \text{ with } \sigma_j \cap \tau \neq \phi \, \}.$$

For a given primal element τ, the local basis functions $\phi_i \in U^h$ for τ are defined by

$$((\phi_i)_e)_j = \delta_{ij}. \tag{6.6.5}$$

Notice that the dimension of U^h on each primal element τ is equal to the number of edges of τ. Thus, the basis functions ϕ_i $(i = 1, 2, \cdots, 12)$ are uniquely determined by (6.6.5). For V^h, the degrees of freedom is given by the set

$$\Sigma^V(\mathbf{v}, \tau) = \{ \, (v_f)_j = \frac{1}{s_j} \int_{\kappa_j} \mathbf{v} \cdot \mathbf{n} \, d\sigma, \ \forall \kappa_j \text{ with } \kappa_j \cap \tau \neq \phi \, \}.$$

For a given primal element τ, the local basis functions ψ_i for τ are defined by

$$((\psi_i)_f)_j = \delta_{ij}. \tag{6.6.6}$$

The set of local basis functions ψ_i ($i = 1, 2, \cdots, 6$) are uniquely determined by (6.6.6) since the dimension of V^h on τ is equal to the number of faces of τ. Let $E \in \mathbb{R}^{M_1}$ and $H \in \mathbb{R}^{F_1}$ be two vectors such that each component of E and H corresponds to each of the degrees of freedoms in Σ^U and Σ^V respectively. We also define a vector $B \in \mathbb{R}^{F_1}$ by $B = \mu H$

Consider a reference primal element $\hat{\tau} = [0, k_1] \times [0, k_2] \times [0, k_3]$. We will perform all computations on $\hat{\tau}$ since the computation on arbitrary primal element can be done by translating the element to $\hat{\tau}$. We will now consider (6.6.4). Let $\hat{\kappa}_i$ be a face of $\hat{\tau}$ parallel to the x- and y-axis and having z-coordinate k_3. Then, we have

$$\hat{\psi}_i = (0, 0, \frac{z}{k_3}).$$

Let κ_i be a primal face parallel to the x-y plane. Taking $\psi^h = \psi_i$ in (6.6.4), we have

$$\sum_{j=r,s} \Big\{ \int_{\tau_j} \mu \mathbf{H}_t^h \cdot \psi_i \, dx + \int_{\tau_j} (\nabla \times \mathbf{E}^h) \cdot \psi_i \, dx \Big\} = 0, \tag{6.6.7}$$

where τ_r and τ_s are two primal elements sharing the same face κ_i. Without loss of generality, we assume that τ_r can be translated to $\hat{\tau}$ with κ_i translated to $\hat{\kappa}_i$. Then, we have

$$\int_{\tau_r} \mu \mathbf{H}_t^h \cdot \psi_i \, dx = \int_{\hat{\tau}} \mu \hat{\mathbf{H}}_t^h \cdot \hat{\psi}_i \, dx = \frac{s_i k_3}{2} \mu \dot{H}_i, \tag{6.6.8}$$

where the last step follows from an application of trapezoidal rule to evaluating the integral on $\hat{\tau}$. Similarly, we have

$$\int_{\tau_r} (\nabla \times \mathbf{E}^h) \cdot \psi_i \, dx = \int_{\hat{\tau}} (\nabla \times \mathbf{E}^h) \cdot \hat{\psi}_i \, dx = \frac{s_i k_3}{2} (\nabla \times \mathbf{E}^h) \cdot \mathbf{n}$$

Since $\nabla \times \mathbf{E}^h$ is a constant,

$$\frac{s_i k_3}{2} (\nabla \times \mathbf{E}^h) \cdot \mathbf{n} = \frac{k_3}{2} \int_{\kappa_i} (\nabla \times \mathbf{E}^h) \cdot \mathbf{n} \, d\sigma = \frac{k_3}{2} (CE_e)_i. \tag{6.6.9}$$

We remark here that similiar results hold for the integrals on τ_s. Using (6.6.8) and (6.6.9) in (6.6.7), we have

$$s_i k_3 \mu \dot{H}_i + k_3 (CE_e)_i = 0, \tag{6.6.10}$$

which is the same as (3.3.6).

Now, we consider (6.6.3). Let $\hat{\sigma}_i$ be an edge of $\hat{\tau}$ parallel to the x-axis and having y-coordinate k_2 and z-coordinate k_3. Then we have

$$\hat{\phi}_i = (\frac{yz}{k_2 k_3}, 0, 0).$$

Let σ_i be an primal edge parallel to the x-axis. Taking $\phi^h = \phi_i$ in (6.6.3), we have

$$\sum_{k=1}^{4} \Big\{ \int_{\tau_{r_k}} \varepsilon \mathbf{E}_t^h \cdot \phi_i \, dx - \int_{\tau_{r_k}} \mathbf{H}^h \cdot (\nabla \times \phi_i) \, dx \Big\} = \sum_{k=1}^{4} \int_{\tau_{r_k}} \mathbf{J} \cdot \phi_i \, dx,$$

where τ_{r_k} $(k = 1,2,3,4)$ are the four primal elements sharing the same edge σ_i. Without loss of generality, we assume τ_{r_1} can be translated to $\hat{\tau}$ with σ_i translated to $\hat{\sigma}_i$. Then, we have

$$\int_{\tau_{r_1}} \varepsilon \mathbf{E}_t^h \cdot \phi_i \, dx = \int_{\hat{\tau}} \varepsilon \mathbf{E}_t^h \cdot \hat{\phi}_i \, dx = \frac{k_1 k_2 k_3}{4} \varepsilon \dot{E}_i,$$

where trapezoidal rule is applied to evaluate the integral on $\hat{\tau}$. Since a similiar result holds for integrals on τ_{r_k} $(k = 2,3,4)$, we have

$$\sum_{k=1}^{4} \int_{\tau_{r_k}} \varepsilon \mathbf{E}_t^h \cdot \phi_i \, dx = k_1 s_i' \dot{E}_i. \tag{6.6.11}$$

Notice that

$$\nabla \times \hat{\phi}_i = (0, \frac{y}{k_2 k_3}, -\frac{z}{k_2 k_3}).$$

Writing $(\mathbf{H}^h)_2$ and $(\mathbf{H}^h)_2$ be the y- and z-component of $\mathbf{H}^h$ respectively, we obtain

$$\int_{\tau_{r_1}} \mathbf{H}^h \cdot (\nabla \times \phi_i) \, dx = \int_{\hat{\tau}} \mathbf{H}^h \cdot (\nabla \times \hat{\phi}_i) \, dx = \int_{\tau_{r_1}} \left\{ (\mathbf{H}^h)_2 \frac{y}{k_2 k_3} - (\mathbf{H}^h)_3 \frac{z}{k_2 k_3} \right\} dx.$$

Applying trapezoidal rule,

$$\int_{\tau_{r_1}} \mathbf{H}^h \cdot (\nabla \times \phi_i) \, dx = k_1 \frac{k_2}{2} H_l - k_1 \frac{k_3}{2} H_s = k_1 \frac{k_2}{2} \frac{1}{\mu} B_l - k_1 \frac{k_3}{2} \frac{1}{\mu} B_s,$$

where H_l corresponds to a primal face κ_l having edge σ_i and normal parallel to the y-axis while H_s corresponds to a primal face κ_s having edge σ_i and normal parallel to the z-axis. Hence,

$$\sum_{k=1}^{4} \int_{\tau_{r_k}} \mathbf{H}^h \cdot (\nabla \times \phi_i) \, dx = k_1 (C' B)_i. \tag{6.6.12}$$

Applying a similiar calculation as that used to get (6.6.11), we have

$$\sum_{k=1}^{4} \int_{\tau_{r_k}} \mathbf{J} \cdot \phi_i \, dx = k_1 s_i' (J_e)_i. \tag{6.6.13}$$

Combining (6.6.11), (6.6.12) and (6.6.13), we see that by using trapezoidal rule, (6.6.3) can be written as

$$k_1 s_i' \dot{E}_i - k_1 (C' H)_i = k_1 s_i' (J_e)_i. \tag{6.6.14}$$

Consequently, if trapezoidal rule is applied to evaluate integrals in (6.6.3)-(6.6.4), we obtain (6.6.10) and (6.6.14), which is a same system as the semi-discrete scheme (3.3.5)-(3.3.6) with a different source term. It is clear from the derivation that the same result holds for discontinuous coefficients and non-uniform grids.

6.2. Unstructured grids. It is now in a position to consider the general case, that is the domain Ω is a polyhedron which is triangulated by tetrahedra. Let τ be a given tetrahedral primal element. Then the finite element space U^h is defined as

$$U^h = \{\mathbf{u}^h \in H_0(\text{curl}, \Omega) \mid \mathbf{u}^h|_\tau = \mathbf{a} + \mathbf{b} \times \mathbf{x}, \text{ for } \mathbf{a}, \mathbf{b} \in \mathbb{R}^3\}, \tag{6.6.15}$$

with the associated set of degrees of freedom given by

$$\Sigma^U(\mathbf{u}, \tau) = \{\ (u_e)_j = \frac{1}{h_j} \int_{\sigma_j} \mathbf{u} \cdot \mathbf{t}\, dl,\ \forall \sigma_j \text{ with } \sigma_j \cap \tau \neq \phi\ \}.$$

For V^h, we have

$$V^h = \{\mathbf{v}^h \in H(\text{div}, \Omega) \mid \mathbf{v}^h|_\tau = \mathbf{c} + d\mathbf{x}, \text{ for } \mathbf{c} \in \mathbb{R}^3, d \in \mathbb{R}\}, \tag{6.6.16}$$

with the associated set of degrees of freedom given by

$$\Sigma^V(\mathbf{v}, \tau) = \{\ (v_f)_j = \frac{1}{s_j} \int_{\kappa_j} \mathbf{v} \cdot \mathbf{n}\, d\sigma,\ \forall \kappa_j \text{ with } \kappa_j \cap \tau \neq \phi\ \}.$$

The local basis functions for (6.6.15) and (6.6.16) are defined in the same way as (6.6.5) and (6.6.6) respectively.

Let τ be a given tetrahedral primal element and $\kappa_j \in \partial\tau$ be a primal face. Denoted by $\mathcal{F}_j$ the tetrahedron formed by the three vertices of κ_j and the circumcenter of τ. Then, on τ, we define

$$\tilde{\psi}_j = \begin{cases} \mathbf{n}_j, & \mathbf{x} \in \mathcal{F}_j \\ 0, & \text{otherwise} \end{cases}$$

Let $\sigma_i \in \partial\tau$ be a primal edge. Denoted by $\tilde{\mathcal{E}}_i$ the polyhedron form by the convex hull of the two vertices of σ_i and all vertices of the dual face κ_i'. Define $\mathcal{E}_i = \tilde{\mathcal{E}}_i \cap \tau$. Then, on τ, we define

$$\tilde{\phi}_i = \begin{cases} \mathbf{t}_i, & \mathbf{x} \in \mathcal{E}_i \\ 0, & \text{otherwise} \end{cases}$$

We emphasis here that $\tilde{\phi}_i$ and $\tilde{\psi}_j$ satisfy (6.6.5) and (6.6.6) respectively.

We will now consider (6.6.4). We will approximate integrals in (6.6.7) in the following way.

$$\int_{\tau_r} \mu \mathbf{H}_t^h \cdot \psi_i\, dx \approx \int_{\tau_r} \mu \tilde{\mathbf{H}}_t^h \cdot \tilde{\psi}_i\, dx,$$

$$\int_{\tau_r} (\nabla \times \mathbf{E}^h) \cdot \psi_i\, dx \approx \int_{\tau_r} (\nabla \times \mathbf{E}^h) \cdot \tilde{\psi}_i\, dx.$$

Here, we use a mass-lumping technique to approximate the integrals. Using the definition of $\tilde{\psi}_i$, we have

$$\int_{\tau_r} \mu \tilde{\mathbf{H}}_t^h \cdot \tilde{\psi}_i\, dx = \mu \dot{H}_i |\mathcal{F}_i| = \mu s_i \dot{H}_i \frac{|\mathcal{F}_i|}{s_i},$$

and since $\nabla \times \mathbf{E}^h$ is a constant on τ_r, we have

$$\int_{\tau_r} (\nabla \times \mathbf{E}^h) \cdot \tilde{\psi}_i \, dx = |\mathcal{F}_i| (\nabla \times \mathbf{E}^h) \cdot \mathbf{n}_i = \frac{|\mathcal{F}_i|}{s_i} \int_{\kappa_i} (\nabla \times \mathbf{E}^h) \cdot \mathbf{n} \, d\sigma.$$

Consequently, we obtain

$$\mu s_i \dot{H}_i \frac{|\mathcal{F}_i|}{s_i} + \frac{|\mathcal{F}_i|}{s_i} (CE_e)_i = 0,$$

which is the same as (3.3.6).

We will now consider (6.6.3). Let τ be a given tetrahedral primal element. Then we approximate integrals in (6.6.3) in the following way.

$$\int_\tau \varepsilon \mathbf{E}_t^h \cdot \phi_i \, dx \approx \int_\tau \varepsilon \tilde{\mathbf{E}}_t^h \cdot \tilde{\phi}_i \, dx = |\mathcal{E}_i| \varepsilon \dot{E}_i = \frac{1}{3} h_i |\kappa_i' \cap \tau| \varepsilon \dot{E}_i,$$

where the last formula for $|\mathcal{E}_i|$ holds because of the orthogonality of primal edge and dual face. Similiarly,

$$\int_\tau \mathbf{J} \cdot \phi_i \, dx \approx \int_\tau \mathbf{J} \cdot \tilde{\phi}_i \, dx = \frac{1}{3} h_i |\kappa_i' \cap \tau| (J_e)_i.$$

Also,

$$\int_\tau \mathbf{H}^h \cdot (\nabla \times \phi_i) \, dx \approx \int_\tau \tilde{\mathbf{H}}^h \cdot (\nabla \times \phi_i) \, dx = \sum_{j=1}^{4} \Big\{ \int_{\mathcal{F}_j} \tilde{\mathbf{H}}^h \cdot (\nabla \times \phi_i) \, dx \Big\}.$$

For each $j = 1, 2, 3, 4$, we compute the above integrals as follows

$$\int_{\mathcal{F}_j} \tilde{\mathbf{H}}^h \cdot (\nabla \times \phi_i) \, dx = \frac{|\mathcal{F}_j|}{s_j} H_j \int_{\kappa_j} (\nabla \times \phi_i) \cdot \mathbf{n} \, d\sigma = \frac{1}{3} |\sigma_j' \cap \tau| \frac{1}{\mu} B_j h_i,$$

if $\mathcal{F}_j$ has a non-empty intersection with the primal edge σ_i. Otherwise, the integral is zero. Consequently, we obtain

$$\varepsilon s_j' \dot{E}_j - (C' B_e')_j = s_j' (J_e)_j.$$

We remark here that the same result holds for discontinuous coefficients.

REFERENCES

[1] A. Chatterjee, L. C. Kempel and J. L. Volakis *Finite element method for electromagnetics: antennas, microwave circuits, and scattering applications.* IEEE Press, 1998.

[2] J. S. Chen and K. S. Yee *The finite-difference time-domain and the finite-volume time-domain methods in solving Maxwell's equations.* IEEE Trans. Antennas Propagat., 45 (1997), pp. 354-363.

[3] Z. Chen, Q. Du and J. Zou. *Finite element methods with matching and non-matching meshes for Maxwell equations with discontinuous coefficients.* SIAM J. Numer. Anal., 37 (2000), pp. 1542-1570.

[4] T. S. Chung and J. Zou. *A finite volume method for Maxwell's equations with discontinuous physical coefficients.* Int. J. Appl. Math., 7 (2001), pp. 201-224.

[5] E. T. Chung, Q. Du and J. Zou. *Convergence analysis on a finite volume method for Maxwell's equations in non-homogeneous media.* SIAM J. Numer. Anal., 41 (2003), pp. 37-63.

[6] P. G. Ciarlet. *The finite element method for elliptic problems.* North-Holland Publishing Company, 1978.

[7] S. Fortune. *Voronoi diagrams and Delaunay triangulations.* Computing in Euclidean geometry, World Scientific, Singapore (1992), pp. 193-233.

[8] V. Girault and P. A. Raviart. *Finite element approximation of the Navier-Stokes equations.* Springer-Verlag, New York, 1979.

[9] M. A. Jensen and Y. Rahmat-Samii. *Finite difference and finite volume time domain techniques in electromagnetics: A comparative study.* Radio Science, 31 (1996), pp. 1823-1836.

[10] J. Jin. *The finite element method in electromagnetics.* John Wiley and Sons, Inc.

[11] R. J. Leveque. *Finite volume methods for hyperbolic problems.* Cambridge University Press, 2002.

[12] N. K. Madsen. *Divergence preserving discrete surface integral methods for Maxwell's curl equations using non-orthogonal unstructured grids.* J. of Comput. Phys., 119 (1995), pp. 34-45.

[13] P. Monk. *Analysis of a finite element method for Maxwell's equations.* SIAM J. Numer. Anal., 29 (1992), pp. 714-729.

[14] P. Monk. *An analysis of Nédélec's method for the spatial discretization of Maxwell's equations.* J. Comput. Appl. Math., 47 (1993), pp. 101-121.

[15] P. Monk and E. Süli. *A convergence analysis of Yee's scheme on nonuniform grids.* SIAM J. Numer. Anal., 31 (1994), pp. 393-412.

[16] J. Nédélec. *Mixed finite element in* $\mathbb{R}^3$. Numer. Math., 35 (1980), pp. 315-341.

[17] R. A. Nicolaides. *Direct discretization of planer div-curl problems.* SIAM J. Numer. Anal., 29 (1992), pp. 32-56.

[18] R. A. Nicolaides and D. Q. Wang. *Convergence analysis of a covolume scheme for Maxwell's equations in three dimensions.* Math. Comp., 67 (1998), pp. 947-963.

[19] R. A. Nicolaides and X. Wu. *Covolume solutions of three-dimensional div-curl equations.* SIAM J. Numer. Anal., 34 (1997), pp. 2195-2203.

[20] D. J. Riley and C. D. Turner. *A solid-model-based, transient volumetric Maxwell-solver using hybrid grids.* IEEE Antennas Propagat. Magazine, 39 (1997), pp. 20-33.

[21] N. O. Sadiku. *Elements of electromagnetics.* Oxford University Press, 2001.

[22] A. Taflove. *Computational electrodynamics.* Artech House, Inc., 1995.

[23] K. S. Yee. *Numerical solution of initial boundary value problems involving Maxwell's equations in isotropic media.* IEEE Trans. Antennas Propagat., 14 (1966), pp. 302-307.